

# ACS Polarization Calibration - I. Introduction and Status Report

---

J. Biretta, V. Kozhurina-Platais, F. Boffi, W. Sparks, and J. Walsh  
June 14, 2004

---

## ABSTRACT

*We review the current status of the ACS polarization calibration. We begin with a brief description of the instrument and the GO science program, and then review pre-flight calibrations as well as the on-orbit data from programs 9586 and 9661. Various key parameters are derived and discussed -- these include the polarizer transmissions, polarization properties of the mirrors and CCDs, the polarizer angles on the sky, and the instrumental polarization. We close with a summary of remaining issues, advice for observers, and a summary of future plans. A forth coming report will present a preliminary calibration for GO data.*

---

## Table of Contents

1. Introduction	3
2. ACS as a Polarimeter	3
3. Scientific Observing Programs	4
4. Challenges, Goals, and Philosophy	5
5. Pre-Launch Calibrations	8
Polarizer Filters Throughputs	8
Polarizer Filter Angles	12
HRC M3 Mirror	19
WFC IM3 Mirror	23
CCDs	25
RAS/HOMS Test at Ball	27
RAS/Cal Test at GSFC	28
6. On-Orbit Calibration	35
Proposal 9586	35
Proposal 9661	46
Proposal 10055	52
7. Discussion	53
Polarizer Angles	54
Instrumental Polarization	56
8. Remaining Issues	64
9. Advice for Observers	66
10. Future Plans	66
11. Summary	67
References	69

## 1. Introduction

Polarimetry is utilized by a small cross-section of the ACS science program on astrophysical problems ranging from Martian surface properties, to magnetic field structure in synchrotron jets, to models for GRB outbursts. While strong polarizations are sometimes seen in astrophysical sources (20% - 40%), more common sources have polarizations of order a few percent. In order to derive the properties of these targets, we must accurately measure small differences between several observations of the target -- small differences which represent the small polarized signal in the presence of the much larger unpolarized component. Moreover, since ACS is not optimized as a polarimeter, it is likely that there will be significant sources of “false” polarization within the instrument, and in many cases this instrumental polarization will be far larger than the astrophysical polarization we are attempting to measure. It is a challenging problem which we now undertake.

Herein we review the status of the polarization calibration as of early 2004. While much of the work remains for the future, it is nonetheless useful to survey the available information and outline areas where further investigation is necessary. We review relevant results from lab tests on ACS components, pre-launch tests on the integrated instrument, as well as preliminary results of early on-orbit calibrations. We use these data to estimate the instrumental polarization, and derive other ingredients necessary for the calibration. The actual calibration of observer science data is a topic left to future reports.

## 2. ACS as a Polarimeter

ACS contains six polarizing filters which are sensitive to linear polarization. There are three visible-light optimized or “VIS” polarizers which are designated POL0V, POL60V, POL120V, and three blue-optimized or “UV” polarizers called POL0UV, POL60UV, and POL120UV. As the names imply, each set has three polarizers set at nominal 60 degree angles to each other. In principle, the linear polarization properties of a target can be derived by making observations through each of the three polarizers in a particular set. These three observations should be sufficient to constrain the three parameters of the target (e.g. the set of I, Q, and U parameters, or the flux, fractional polarization, and polarization position angle).

The VIS polarizers (POLV, POL\_V, or POLnV set) are located in filter wheel 2 and employ an “HN32” polaroid. They will typically be used in conjunction with a spectral filter in wheel 1 which include F475W\*, F502N, F550M, F555W, F606W\*, F625W\*, F658N\*, F775W\*, F850LP, and F892N (“\*” denotes a filter whose use with the polarizers is considered to be “supported”).

The three UV polarizers (POLUV, POL\_UV, POLnUV set) are located in filter wheel 1, and are coated with “Polacoat 105UV.” These will generally be used in conjunction with a

spectral filter in filter wheel 2 which include F220W\*, F250W\*, F330W\*, F344N, F435W\*, F660N, and F814W\* (again “\*” denotes a supported filter combination).

The polarizer filters may be used with either the HRC or WFC channels. Since they are “small filters” they fully illuminate the entire field-of-view only for the HRC, and illuminate a little less than one quadrant of the WFC. Hence, when used with the WFC channel the TRANS scheduling software defaults to placing the target on the outer quadrant of WFC1 near pixel (3096, 1024) and reading out only that 2048x2048 quadrant of the detector. An alternate targeting on WFC2 near pixel (1048,1024) can be invoked using engineering-only commands. These positionings are controlled by the SIAF file.

### 3. Scientific Observing Programs

While there are a large number of potential combinations of polarizer, spectral filter, and imaging channel, in practice only a small subset has been used to date. In the interest of saving effort, we will concentrate our work on the most popular combinations. Table 1 summarizes the ACS polarization science program as of May 2004<sup>1</sup>. As can be seen, most

**Table 1.** ACS Polarization GO Program

Cycle	Program	PI	Channel	Modes Used
11	9299	Ford (GTO)	HRC WFC WFC	POLUV+F435W POLV+F475W POLV+F775W
11	9385	Lemon	HRC	POLUV+F220W POLUV+F250W POLUV+F330W POLUV+F435W POLV+F625W POLV+F658N POLV+F775W
11	9493	Capetti	HRC	POLUV+F330W POLV+F606W
11	9405	Fruchter	WFC	POLV+606W
12	9738	Bell	HRC	POLUV+F250W POLUV+F330W POLUV+F435W POLUV+F814W
12	9787	Hester	WFC	POLV+F606W
12	9829	Biretta	HRC	POLV+F606W
12	9847	Perlman	WFC	POLV+F606W
13	10133	Biretta	HRC	POLV+F606W
13	10178	Hines	HRC	POLV+F606W

**Table 1.** ACS Polarization GO Program

Cycle	Program	PI	Channel	Modes Used
13	10262	Humphreys	HRC	POLV+F606W

of the modes involve the HRC, and F606W is the most commonly used filter. Nearly all the usage involves wide band (W) filters, with the only exception of F658N. The WFC has only been used with POLV together with F475W, F606W, and F775W. The above proposal list may be condensed into a list of unique modes as shown in Table 2. This list is

**Table 2.** ACS Polarization Modes in Use (5/2004)

Channel	Polarizer Set	Spectral Filters
HRC	POLUV	F220W F250W F330W F435W F814W
	POLV	F606W F625W F658N F775W
WFC	POLV	F475W F606W F775W

essentially identical to the list of “supported” filter combinations given in the ACS Instrument Handbook.

#### 4. Challenges, Goals, and Philosophy for ACS Polarization Calibration

Below we review some of the challenges, and potential issues which may need to be addressed during calibration of ACS polarimetry. Since the design of ACS is firstly optimized for high-efficiency wide-field imaging, and polarimetry had only secondary or tertiary importance, we should not be surprised if it offers more challenges than an instrument specifically designed for polarimetry.

1. Instrumental polarization and mirrors: A potential issue for ACS polarimetry is the use of metal-film mirrors in the optical chain. Both the HRC and WFC optical chains contain 3 mirrors which are located between the instrument entrance aperture and the polarizer filters. The first two mirrors in each chain are used near normal incidence and should have modest effects, but the third mirror has a 45 to 50

---

1. This table may be somewhat inaccurate, as observers often change strategy.

degree incidence angle and could potentially have large effects on the polarization properties of the incident light. Such mirrors typically have different reflectivities for light polarized parallel and perpendicular to the plane of incidence -- an effect known as “diattenuation” -- and hence will cause different intensities to be recorded in the different polarizer filters for reasons which have nothing to do with the celestial target (i.e. instrumental polarization). Diattenuation will also alter the polarization angles of celestial targets. “Phase retardation” is another potential effect arising in metal film mirrors -- incident light which is linearly polarized in neither the plane of incidence, nor perpendicular to the plane of incidence, will be converted to elliptically polarized light. In other words, some part of the energy will be converted to circular polarization, to which the linear polarizer filters are insensitive. Both diattenuation and phase retardance effects will vary as the HST roll angle changes relative to the polarization angle of the celestial target. The diattenuation effects will vary from maximum to minimum over a 90 degree rotation, while phase retardance effects will vary from maximum to minimum over a 45 degree rotation. Since the optics of the WFC and HRC channels are significantly different with regards to mirror coatings (and to a lesser degree the mirror angles), we anticipate they will have completely different calibrations.

2. Instrumental polarization and CCD detectors: Another unique aspect of ACS is the use of strongly tilted detectors in the optical design, which may introduce additional polarization effects similar to those seen in metallic mirrors. A primary goal of the calibration will be to assess these potential effects, and then find a way to accurately removed them from observer data.
3. Throughputs of the polarizers: While the throughputs of the polarizers have been measured in pre-flight ground tests, it would be useful to have an independent on-orbit measurement of their throughputs, as is normally done for the spectral filters. This implies measurement of the transmission of each of the six physical filters as a function of wavelength for light polarized in both the parallel and perpendicular directions. The UV polarizer set appears to have significant leakage of cross-polarized light, and we will need to include corrections for this during calibration.
4. Orientation of the polarizers: While the polarizers have supposedly been mounted in the instrument filter wheels at exactly 60 degree rotations, it would be useful to have an independent, on-orbit test of the actual orientations of the six filters. Furthermore, it would be useful to verify the absolute orientations with respect to the spacecraft axes, so that target polarization properties maybe confidently derived in terms of “position angle” on the celestial sphere.
5. Flat field accuracy: Many GO observations will want to derive the polarization properties of targets which extend over much of the instrument’s field-of-view (e.g. nova light echoes, reflection nebulae, extragalactic jets, etc.) hence it is desirable to know how the calibration varies across the detector. Many of the planned calibrations involve observation of a standard star at only a single location (aperture center), hence some special attention may be needed to validate the calibration over a wider area. Some particular concern arises because ACS will use two filters for polarimetry (the spectral filter and the polarizer) which are in close proximity and

hence susceptible to reflections between these filters. While the direct impact on raw science data is likely minimal, there is a significant potential for flat field calibration images to be corrupted, since the entire field-of-view is illuminated (e.g. ground test flats, Earth flats). This will in turn lead to corruption of calibrated science data.

6. Determination of the unvignetted field: The ACS polarizers were designed as “small filters” and hence illuminate only a small region of the ACS WFC field-of-view. It would be useful to accurately delineate the unvignetted region in the focal plane, so that observers could avoid the vignetted regions. It may be possible to recover some information for images in the vignetted regions through proper flat field calibration.
7. Geometric distortion: The ACS polarizers contain a small amount of optical power (i.e. the filters include a weak lens) to avoid defocussing of images caused by the extra glass path when the polarizers are in the optical beam. This lens also introduces a small amount of geometric distortion which must be corrected when comparing polarizer and non-polarizer images of the same target. This distortion correction must also preserve photometric accuracy for both point and extended sources. As we will later see, there is an additional patchy or small-scale distortion caused by ripples in the polaroid material.
8. Evolution with time: It is conceivable that the polarization calibration might vary or degrade with time. There is probably little on-orbit experience with polaroid filters, and one must consider the possibility of unexpected degradation due to either vacuum exposure, surface damage, or radiation damage.

In a more general sense, the goal of the calibration is to be able to accurately predict the counts measured by the detector for a given celestial object, and of course, to invert this relationship and derive the source properties from the observed counts. This calibration will depend on the detailed properties of each optical element in the system. For the mirrors (and also detectors) in the system, the calibration will depend on the incidence angle, the reflectance for both parallel and perpendicular polarizations, and the amount of phase retardance at each wavelength. For the polarizers, the important quantities are the filter rotation, and the parallel and perpendicular transmissions. Given the many optical elements with polarization effects, it is likely the detected counts will have a very complex relationship to properties of the celestial target.

Ideally, the individual optical components would be well characterized by laboratory testing, and then followed-up by aggressive lab calibration of the assembled instrument. On-orbit calibration, which uses valuable HST time, would merely provide a quick confirmation of ground calibration. So far the on-orbit calibration program has been largely based on this approach -- the assumption that most parameters of the system were well-characterized on the ground. However, it remains to be seen whether there is in fact adequate pre-launch data, and whether there is agreement between the pre- and post-launch tests. If

significant deficiencies are found, or discrepancies arise between the ground and on-orbit results, it may be necessary to conduct a much more intensive campaign of on-orbit calibration to effectively supplement or replace the pre-launch tests.

## 5. Pre-Launch Calibrations

Prior to integration and installation of ACS into HST, a number of calibrations and tests were performed on the ground of both individual optical components and of the completed ACS. We briefly review these here.

### *Polarizer Filters*

ACS has two sets of polarizers. There are three “visible” polarizers set at 60 degree angles to each other, and three “UV” polarizers also set at 60 degree angles. Both sets use dichroic polymer type polarizer filters. These are sheets of a polymer, usually polyvinyl-alcohol, which have been stretched uni-directionally hence producing highly elongated molecular chains. These are then treated with iodine, leading to the formation of long chains of polymeric iodine. The resulting sheet has high transmission for light linearly polarized perpendicular to the stretch direction, and high absorption for light polarized parallel to the stretch. (This information will be useful later when we examine the optical distortion caused by the polarizer filters.) For the visible set, a standard preparation known as HN-32 was used (Meadowlark Corporation), and 105UV Polacoat (Sterling Optics Corp.) was used for the UV set. These materials are bonded inside thick positive meniscus lenses, which both provide mechanical protection and maintain proper focussing of light at the CCD surface. Some further details of the polarizers can be found in Woodruff, 1996A and 1996B.

Laboratory measurements of the polarizer throughputs were made by D. Leviton at GSFC in 1998 prior to their integration into ACS. Table 3 and Table 4 show the parallel and per-

**Table 3.** POLVIS Filter Transmissions from Ground Tests

Wave-length (nm)	POL0V		POL60V		POL120V		Average across polarizers			
	T <sub>par</sub>	T <sub>perp</sub>	T <sub>par</sub>	T <sub>perp</sub>	T <sub>par</sub>	T <sub>perp</sub>	T <sub>par</sub>		T <sub>perp</sub>	
							Avg	σ	Avg	σ
350	0.148	5.0E-05	0.141	1.3E-04	0.168	4.6E-05	0.152	0.014	7.4E-05	4.5E-05
375	0.135	1.8E-04	0.122	2.4E-04	0.133	1.5E-04	0.130	0.007	1.9E-04	5.0E-05
400	0.281	2.7E-04	0.262	4.0E-04	0.290	2.3E-04	0.277	0.014	3.0E-04	8.8E-05
425	0.387	2.3E-04	0.386	4.5E-04	0.412	1.8E-04	0.395	0.015	2.9E-04	1.4E-04

**Table 3.** POLVIS Filter Transmissions from Ground Tests

Wave-length (nm)	POL0V		POL60V		POL120V		Average across polarizers			
	T <sub>par</sub>	T <sub>perp</sub>	T <sub>par</sub>	T <sub>perp</sub>	T <sub>par</sub>	T <sub>perp</sub>	T <sub>par</sub>		T <sub>perp</sub>	
							Avg	σ	Avg	σ
450	0.475	1.1E-04	0.446	4.1E-04	0.486	9.3E-05	0.469	0.021	2.0E-04	1.8E-04
475	0.518	6.1E-05	0.534	3.9E-04	0.530	7.3E-05	0.527	0.008	1.7E-04	1.9E-04
500	0.508	1.3E-05	0.498	1.2E-04	0.520	2.1E-05	0.509	0.011	5.2E-05	5.9E-05
525	0.517	1.2E-05	0.500	1.0E-04	0.517	1.7E-05	0.511	0.010	4.4E-05	5.2E-05
550	0.492	1.1E-05	0.469	9.4E-05	0.485	1.7E-05	0.482	0.012	4.1E-05	4.6E-05
575	0.489	9.2E-06	0.488	7.5E-05	0.479	1.5E-05	0.485	0.006	3.3E-05	3.6E-05
600	0.478	8.5E-06	0.480	6.0E-05	0.501	1.5E-05	0.486	0.013	2.8E-05	2.8E-05
625	0.489	8.1E-06	0.489	5.4E-05	0.503	1.4E-05	0.493	0.008	2.5E-05	2.5E-05
650	0.497	7.9E-06	0.504	5.1E-05	0.541	1.4E-05	0.514	0.023	2.4E-05	2.3E-05
675	0.490	7.6E-06	0.559	4.5E-05	0.541	1.4E-05	0.530	0.036	2.2E-05	2.0E-05
700	0.548	8.1E-06	0.584	4.7E-05	0.573	1.6E-05	0.568	0.019	2.4E-05	2.0E-05
725	0.595	6.3E-06	0.573	3.7E-05	0.604	1.2E-05	0.591	0.016	1.8E-05	1.6E-05
750	0.589	2.9E-05	0.633	5.0E-05	0.629	3.8E-05	0.617	0.024	3.9E-05	1.1E-05
775	0.660	7.1E-04	0.642	5.4E-04	0.652	8.2E-04	0.652	0.009	6.9E-04	1.4E-04
800	0.664	9.9E-03	0.675	7.4E-03	0.693	9.8E-03	0.678	0.015	9.0E-03	1.4E-03
825	-	-	-	-	0.582	1.8E-01	-	-	-	-

**Table 4.** POLUV Filter Transmissions from Ground Tests

Wave-length (nm)	POL0UV		POL60UV		POL120UV		Average across polarizers			
	T <sub>par</sub>	T <sub>perp</sub>	T <sub>par</sub>	T <sub>perp</sub>	T <sub>par</sub>	T <sub>perp</sub>	T <sub>par</sub>		T <sub>perp</sub>	
							Avg	σ	Avg	σ
250	0.291	0.0068	0.292	0.0099	0.274	0.0064	0.286	0.010	0.0077	0.0019
280	0.395	0.022	0.400	0.028	0.379	0.022	0.391	0.011	0.024	0.0030
290	0.410	0.028	0.421	0.034	0.399	0.028	0.410	0.011	0.030	0.0034
300	0.435	0.034	0.441	0.041	0.422	0.035	0.433	0.010	0.037	0.0038
310	0.450	0.037	0.463	0.042	0.442	0.037	0.451	0.011	0.039	0.0031
320	0.465	0.039	0.454	0.045	0.454	0.039	0.458	0.007	0.041	0.0038
330	0.480	0.042	0.495	0.045	0.470	0.042	0.482	0.012	0.043	0.0021

**Table 4.** POLUV Filter Transmissions from Ground Tests

Wave-length (nm)	POL0UV		POL60UV		POL120UV		Average across polarizers			
	T <sub>par</sub>	T <sub>perp</sub>	T <sub>par</sub>	T <sub>perp</sub>	T <sub>par</sub>	T <sub>perp</sub>	T <sub>par</sub>		T <sub>perp</sub>	
							Avg	$\sigma$	Avg	$\sigma$
340	0.489	0.047	0.509	0.050	0.477	0.048	0.492	0.016	0.048	0.0013
350	0.507	0.055	0.527	0.057	0.493	0.057	0.509	0.017	0.056	0.0016
360	0.530	0.058	0.534	0.061	0.497	0.060	0.520	0.020	0.060	0.0017
370	0.502	0.053	0.537	0.060	0.515	0.056	0.518	0.017	0.056	0.0038
380	0.511	0.051	0.540	0.060	0.519	0.054	0.523	0.015	0.055	0.0048
390	0.491	0.041	0.543	0.047	0.528	0.041	0.520	0.027	0.043	0.0034
400	0.521	0.038	0.538	0.044	0.520	0.036	0.526	0.010	0.039	0.0039
450	0.519	0.008	0.522	0.011	0.562	0.005	0.534	0.024	0.008	0.0032
500	0.549	0.008	0.535	0.012	0.538	0.005	0.541	0.007	0.009	0.0034
550	0.557	0.009	0.563	0.016	0.589	0.008	0.569	0.017	0.011	0.0041
600	0.561	0.006	0.554	0.013	0.579	0.005	0.564	0.013	0.008	0.0042
650	0.582	0.018	0.578	0.026	0.603	0.014	0.588	0.013	0.019	0.0061
700	(0.418)	0.114	0.612	0.068	0.630	0.041	0.607	0.026	0.075	0.0366
750	0.599	0.112	0.660	0.114	0.611	0.095	0.623	0.032	0.107	0.0104
800	0.650	0.200	0.636	0.210	0.663	0.168	0.650	0.013	0.193	0.0219
850	0.616	0.310	0.615	0.311	0.654	0.258	0.628	0.022	0.293	0.0305

pendicular transmission values,  $T_{\text{par}}$  and  $T_{\text{perp}}$ , taken from Leviton's Excel spreadsheet. The results for the POL0, POL60, and POL120 filters are given as a function of wavelength. No results were given shortwards of 250 nm; and only POL120V was measured at 825 nm. The results were reputed to have been identical for the different polarizers to within the measurement errors, so the dispersion in results across the different polarizers is probably an indicator of the measurement accuracy. The average value and dispersion,  $\sigma$ , across the polarizers are given in the right columns. (Some of this information can also be found at [http://acs.pha.jhu.edu/instrument/filters/data/pol\\_vis.dat](http://acs.pha.jhu.edu/instrument/filters/data/pol_vis.dat) and [http://acs.pha.jhu.edu/instrument/filters/data/pol\\_uv.dat](http://acs.pha.jhu.edu/instrument/filters/data/pol_uv.dat).)

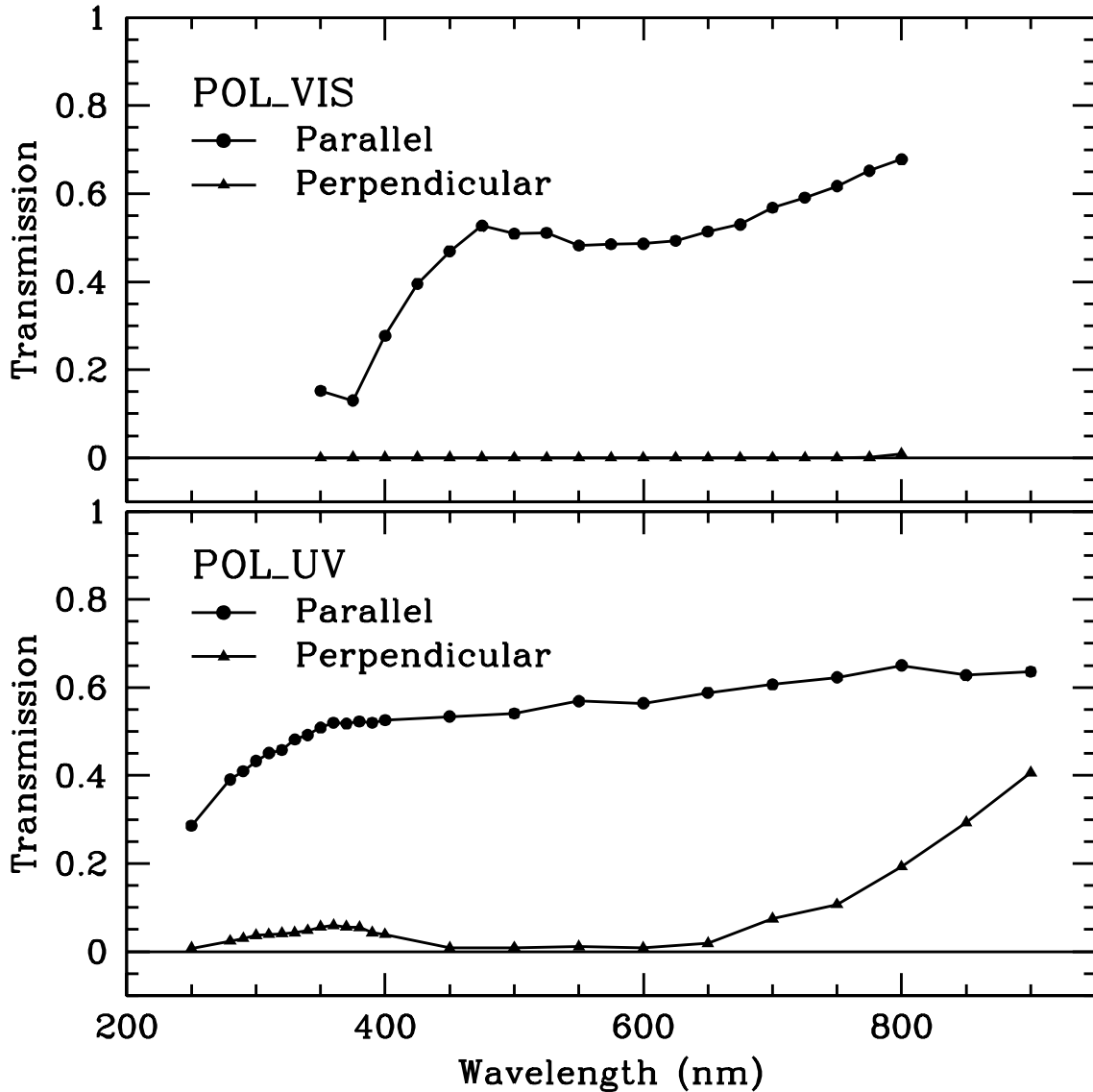
One result deserves additional discussion. For the POL0UV filter the parallel transmission at 700nm appears anomalously low, with a value of 0.418 vs. values of 0.612 and 0.630 for POL60UV and POL120UV, respectively. Each of the numbers in this Table is the average of measurements made with the measurement apparatus along and perpendicular to the

principle axes of the illuminator -- this was done in an attempt to average out any spurious polarization in the light source. Hence the value 0.418 is the average of two numbers, a value of 0.270 for the “TUT dominant” axis and 0.566 for “perpendicular to TUT dominant” axis. Of these two numbers, only the former appears anomalous and very different from neighboring wavelengths (e.g., 0.592 at 650 nm and 0.593 at 750 nm), while the later is similar to adjacent wavelengths (e.g., 0.572 at 650 nm and 0.606 at 750 nm). Hence it appears likely that this low value for POL0UV at 700 nm merely reflects some sort of measurement error for the “TUT dominant” axis, rather than any real issue in the POL0UV polarizer. As such, we have ignored the low value of 0.270 for the “TUT dominant” axis, and instead interpolated across adjacent wavelengths for the “TUT dominant” axis when computing the average  $T_{\text{par}}$  across the different UV polarizers at 700 nm. The uncorrected value would have been 0.553, while the corrected value we will use is 0.607.

The parallel and perpendicular transmissions averaged across each filter set are shown in Figure 1. The VIS polarizer set appears to have excellent rejection of cross-polarized light,

while the UV polarizers have significant leakage, especially at near-UV and far-red wavelengths.

**Figure 1:** Averaged throughputs of ACS polarizer filters (pre-launch measurements).



***Polarizer Filter Angles***

The projected angles of the polarizer filter E-vectors on the sky are a very important parameter in their calibration. Since this has not been described elsewhere, we will

attempt to derive the angles from the instrument design specifications. Figure 2 and Figure 3 show the two ACS filter wheels as viewed from the CCD side (Gracey 1997). The first filter wheel contains the three UV polarizers in slots 8, 9, and 10, while the second filter wheel contains the three VIS polarizer in slots 8, 10, and 12. As can be seen on the drawings, the zero angle polarizers are nominally oriented parallel to the filter wheel tangent, while the 60 and 120 degree filters are rotated clockwise by their nominal angles. Due to the apparent inversion caused by the IM3 and M3 mirrors, this will be opposite the apparent rotations on the sky. In other words, if the zero angle polarizers were oriented north-south, the 60 and 120 degree polarizers would be oriented at position angles 60 and 120 degrees, respectively.

Orienting the filter wheel on the sky is somewhat more challenging. Figure 4 was provided by George Hartig (private communication) and shows the apparent orientation of the ACS detectors relative to one of the ramp filters. While the view in the figure is looking towards the detector, the configuration is the same as the projection on the sky, due to the inversion by the IM3 and M3 mirrors. On this drawing we can measure the angle between the HRC edge between the C and D amplifiers (also known as the HRC +X axis), and the filter wheel tangent. The result is that the angle from the HRC +X axis to the filter wheel tangent is 15.5 degrees counter-clockwise.

**Figure 2:** Schematic drawing of filter wheel 1 showing orientation of the UV polarizers.

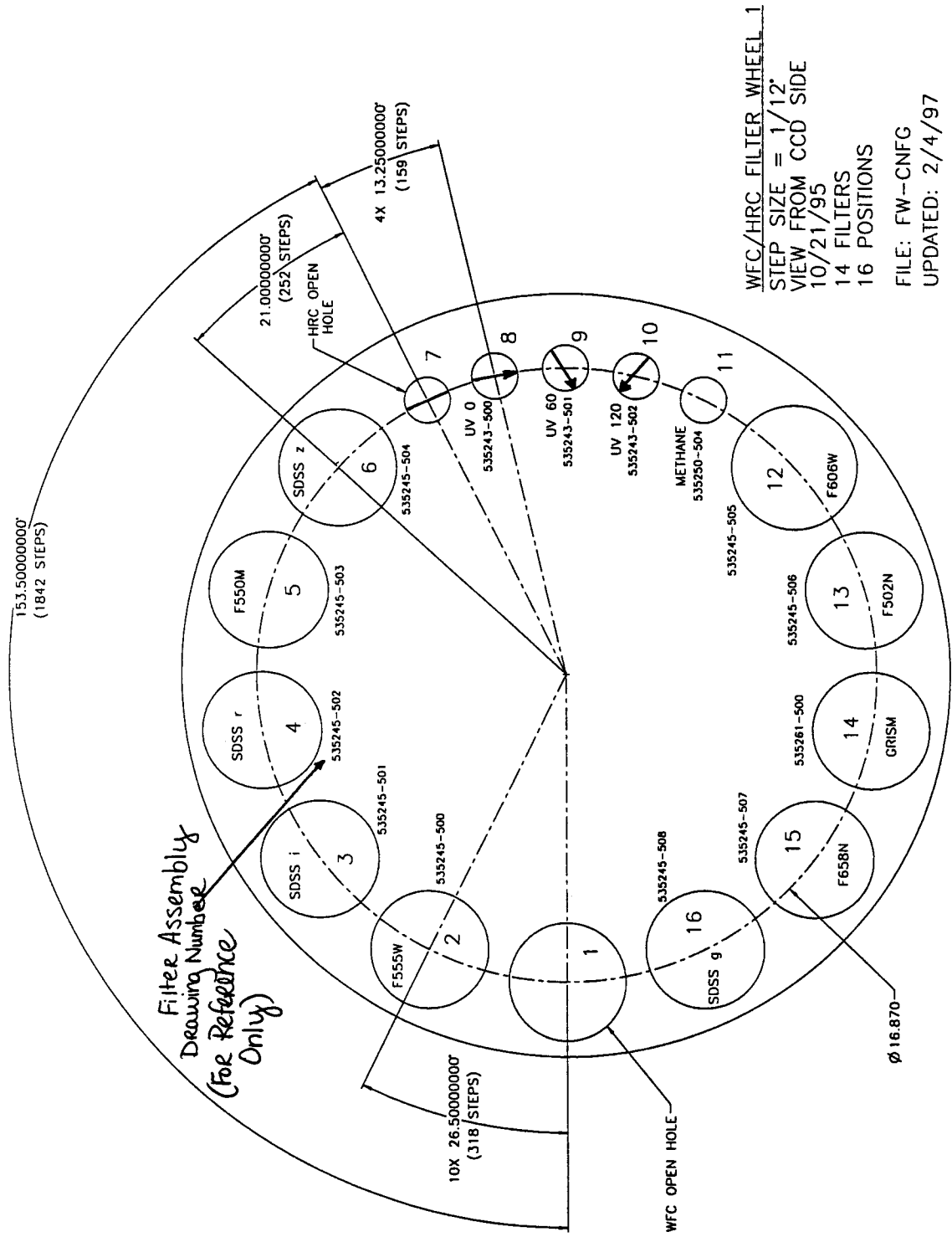


**Figure 3:** Schematic drawing of filter wheel 2 showing orientation of the VIS polarizers.

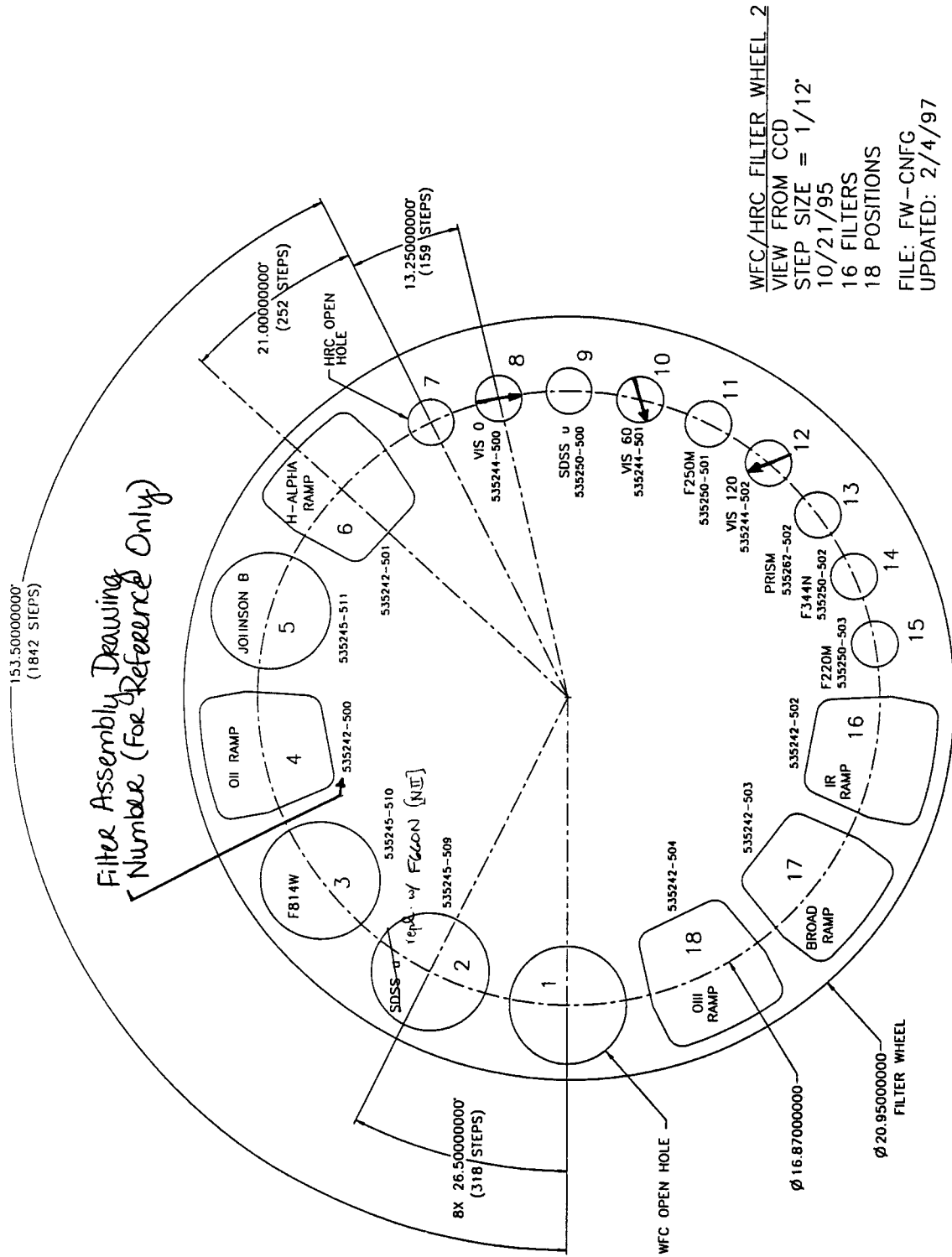
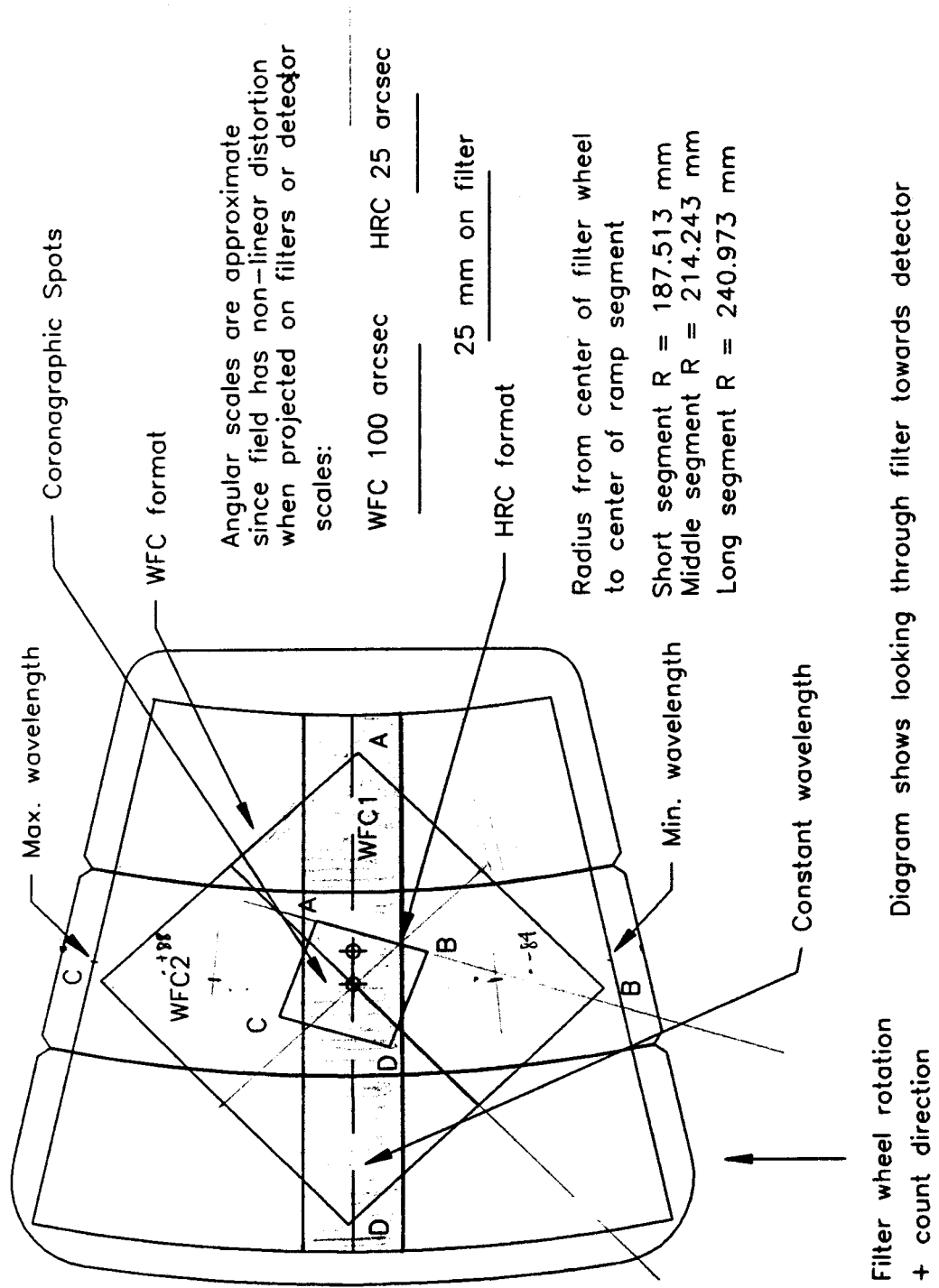


**Figure 4:** Schematic drawing showing HRC and WFC superposed on a ramp filter.



Finally, we need to know the orientation of the HRC +X axis on the sky. This is given in the ACS Instrument Handbook (Version 4.0, Ch. 8). The angle from the spacecraft V3 axis to the HRC +X axis, also known as  $\beta_x$ , is -84.1 degrees counter-clockwise. Hence the “per design” polarizer filter angles on the sky for the HRC are as summarized in Table 5. The parameter PA\_V3, the position angle of the spacecraft V3 axis, is usually contained in the data headers.

**Table 5.** Derivation of HRC polarizer angles using method #1: HRC in Figure 4.

Parameter	Angle (degrees counter-clockwise projected on sky)		
	POL0	POL60	POL120
Spacecraft V3 axis position angle on sky	PA_V3		
V3 to HRC +X axis	-84.1		
HRC +X axis to filter wheel tangent	15.5		
Polarizer to filter wheel tangent	0	60	120
Result: PA of polarizer on sky	PA_V3 - 68.6	PA_V3 - 8.6	PA_V3 + 51.4

An alternate derivation (method #2) might use the WFC as depicted in Figure 4. On Figure 4 the angle from the WFC chip gap line to the filter wheel tangent is 44.2 degrees counter-clockwise. The angle from the spacecraft V3 axis to the WFC +X direction (X-axis angle) at the WFCENTER aperture is 92.1 degrees (from ACS Instrument Handbook). We must also allow for the fact that the filter wheel undergoes a rotation between positioning a filter in front of the WFC and in front of the HRC. This rotation is 153.5 degrees (1842 steps), which can be deduced from Figure 2 -- a counter-clockwise (clockwise on the sky) rotation is needed to move the HRC clear slot to the position of the WFC clear slot. Table 6 summarizes the calculation. Thus the result for the zero-angle polarizer

**Table 6.** Derivation of HRC polarizer angles by method #2: WFC chip gap in Figure 4.

Parameter	Angle (degrees counter-clockwise projected on sky)		
	POL0	POL60	POL120
Spacecraft V3 axis position angle on sky	PA_V3		
V3 to WFC +X axis (at chip gap)	92.1		
WFC +X axis (at chip gap) to filter wheel tangent	44.2		
Rotate filter wheel from WFC to HRC	153.5		
Filter wheel tangent to polarizer angle	0	60	120

**Table 6.** Derivation of HRC polarizer angles by method #2: WFC chip gap in Figure 4.

Parameter	Angle (degrees counter-clockwise projected on sky)		
	POL0	POL60	POL120
Result: PA of polarizer on sky	PA_V3 - 70.2	PA_V3 - 10.2	PA_V3 + 49.8

(POL0) is -68.6 degrees when computed using the HRC drawing, and -70.2 degrees using the WFC drawing. The difference of 1.6 degrees is probably indicative of the uncertainty (or at least a lower limit to the uncertainty) in this approach. For now, we will adopt the average value of methods #1 and #2. *Hence for the HRC the zero-angle polarizer E-vector is at position angle PA\_V3 - 69.4 degrees on the sky, with an uncertainty of 1 degree.*

Once we have an angle on the sky for a polarizer filter used with the HRC, it is fairly straight forward to calculate the angle for the same filter used with the WFC. As mentioned above, when the WFC is utilized, the filter wheel is rotated by 153.5 degrees (1842 steps) to move a filter from the HRC center to the center of the WFC. Additionally, there is a small rotation of 57 steps or 4.75 degrees which is needed to move the filter from the WFC center to the aperture position used for the polarizer filter (Welty, private communication). Since the polarizers are small filters, they are usually placed in front of one quad of the WFC detector set. The default position is near the center of the B amplifier quad on WFC1 at pixel (x,y)=(3096,1024). This small rotation is in the opposite direction from the large HRC to WFC rotation. Hence the polarizer angles for the WFC can be obtained by subtracting 148.75 degrees from the HRC angles. This is summarized in Table 7. *Hence for the WFC the zero-angle polarizer E-vector is at position angle PA\_V3 - 38.15 degrees on the sky, with an uncertainty of 1 degree.*

**Table 7.** Derivation of polarizer angles for the WFC using the HRC result.

Parameter	Angle (degrees counter-clockwise projected on sky)		
	POL0	POL60	POL120
PA of polarizer on sky for HRC	PA_V3 - 69.4	PA_V3 - 9.4	PA_V3 + 50.6
Rotate filter wheel from HRC to WFC	-153.5		
Rotate filter wheel from WFC center to WFC1 pixel (3096,1024)	4.75		
Result: PA of polarizer on sky	PA_V3 - 218.15	PA_V3 - 158.15	PA_V3 - 98.15

***HRC M3 Mirror***

Mirrors within the ACS camera are a likely source of instrumental polarization, especially the M3 and IM3 mirrors which are placed at large incidence angles (Walsh 2001).

The HRC M3 mirror is placed at an incidence angle of 47.9 degrees. Its coating is specified as aluminum (approx 650 Angstroms) over-coated with 606 Angstroms of  $\text{MgF}_2$ . No direct measurements were made of its polarization properties prior to installation in ACS, hence it will be necessary to calculate its properties using basic physics. Simple reflectivity measurements were made on a witness sample and these can be used as a consistency check on computed models. Table 8 lists these reflectivity  $R$  measured for the ACS M3-1 flight mirror witness AMC9616 at Ball (Sullivan 1997). An incidence angle of 48.9 degrees was used for the measurements, which is close to the ACS design angle.

Given the materials and thicknesses discussed above, it is possible to compute the polarization properties using equations and physical constants given in Biretta and McMaster (1997). The results are listed in Table 8 and plotted in Figure 5. The calculations were performed assuming an incidence angle of 47.9 degrees and a  $\text{MgF}_2$  thickness of 606 Angstroms. We have ignored the finite thickness of the Aluminum layer, but this should not introduce significant errors as the light intensity is reduced by a factor of approx.  $10^{-4}$  at the rear Aluminum / substrate boundary due to extinction within the Aluminum. The values of  $R_{\text{avg}}$  in Table 8 are the reflectivity for unpolarized light, and should be equivalent to the lab measurements performed on the witness sample.  $R_s$  and  $R_p$  are the reflectivities for light polarized with the E-vector parallel to the *surface*, and parallel to the *plane* of incidence, respectively. The second to last column lists the computed induced polarization  $P$  defined as  $(R_s - R_p)/(R_s + R_p)$ . The final column lists the computed phase retardance angle  $\Delta\phi$  which will be needed later to accurately model ACS.

The measured reflectance value  $R$  and the average calculated value  $R_{\text{avg}}$  agree to about 2% at 2000 Angstroms and above. This provides some reassurance that the calculations are valid, though it would be nice if the agreement were closer<sup>1</sup>. Sullivan 1997 contains a note that the “reflectivity is actually 2% lower” suggesting there are systematic errors present of about this size in the measurements. In any case, the calculated polarization values  $P$  should give some indication of the spurious polarization introduced by the M3 mirror. The

---

1. We note that our computed values of  $R_{\text{avg}}$  and  $P$  in Table 8 are in somewhat poor agreement with computed values given by Woodruff 1996C (differences of 0.5%) but are in excellent agreement with computed  $P$  values given by Hueser 1996 (differences <0.05%); apparently there is some unexplained variation between computed models. We have also verified our calculations against the ZEMAX optical design package, and they are in excellent agreement (differences <0.05%). The low measured reflectances at wavelengths below 2000 Angstroms might be attributed to measurement errors or contamination.

values P range from near-zero around 4000 Angstroms to a high of 5.2% around 8400 Angstroms.

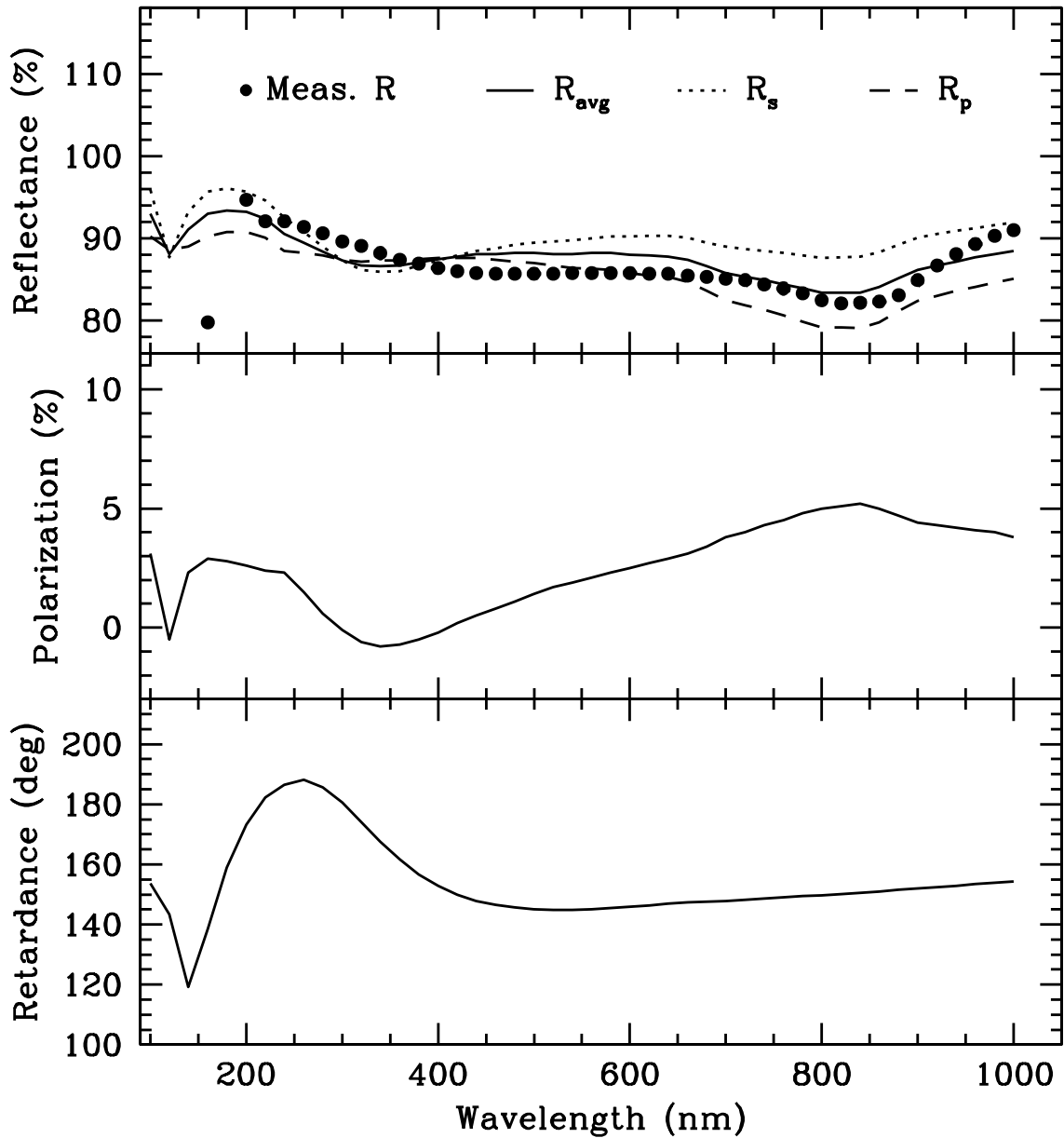
The computed phase retardance ranges from about 180 degrees (same as for a mirror used at normal incidence) to about 145 degrees near 5400 Angstroms. (We ignore lower values in the far-UV since they are not important for HRC.) The loss of linearly polarized intensity is related to the  $M_{33}$  and  $M_{34}$  terms of the Mueller matrix for mirrors (Biretta and McMaster 1997). For the above phase retardance, the loss of linearly polarized intensity is  $(\sin 145^\circ)^2$  or about 33%. Hence we can expect the phase retardance to have a very significant impact on results for polarized targets.

This loss of linear polarization will also have a strong dependence on the HST roll angle relative to the polarization direction of the target. The effect of the phase retardance will be largest when the incident light is polarized in a direction 45 degrees to the principle axes of the tilted M3 mirror, but there will be no effect when the light is polarized along one of the principle axes. Hence the phase retardance effects will vary from maximum to minimum over a 45 degree change in the HST roll angle.

**Table 8.** Properties of HRC M3 Mirror.

Wavelength (Angstroms)	Measured	Calculated Model				
	R	R <sub>avg</sub>	R <sub>s</sub>	R <sub>p</sub>	P	$\Delta\phi$ (degrees)
1000		0.930	0.959	0.902	0.031	153.776
1200	0.656	0.881	0.877	0.886	-0.005	143.409
1400	0.642	0.911	0.932	0.890	0.023	119.121
1600	0.798	0.930	0.957	0.902	0.029	138.590
1800	-	0.934	0.961	0.908	0.028	158.919
2000	0.947	0.932	0.957	0.908	0.026	173.335
2200	0.921	0.924	0.946	0.901	0.024	182.309
2400	0.921	0.905	0.925	0.885	0.023	186.517
2600	0.914	0.895	0.908	0.882	0.015	188.168
2800	0.906	0.884	0.890	0.879	0.006	185.642
3000	0.896	0.873	0.873	0.874	-0.001	180.544
3200	0.891	0.867	0.862	0.872	-0.006	174.103
3400	0.882	0.866	0.859	0.873	-0.008	167.606
3600	0.874	0.867	0.860	0.873	-0.007	161.696
3800	0.869	0.871	0.867	0.875	-0.005	156.711
4000	0.864	0.875	0.873	0.876	-0.002	152.821
4200	0.860	0.878	0.879	0.876	0.002	149.928
4400	0.858	0.881	0.885	0.876	0.005	147.860
4600	0.857	0.881	0.888	0.874	0.008	146.474
4800	0.857	0.882	0.892	0.872	0.011	145.624
5000	0.857	0.882	0.895	0.870	0.014	145.148
5200	0.857	0.881	0.896	0.867	0.017	144.927
5400	0.858	0.881	0.898	0.864	0.019	144.925
5600	0.858	0.882	0.900	0.863	0.021	145.118
5800	0.858	0.882	0.902	0.862	0.023	145.436
6000	0.858	0.880	0.902	0.858	0.025	145.858
6200	0.857	0.879	0.903	0.855	0.027	146.362
6400	0.857	0.878	0.903	0.853	0.029	146.910
6600	0.855	0.874	0.901	0.847	0.031	147.321
6800	0.853	0.866	0.895	0.836	0.034	147.593

Wavelength (Angstroms)	Measured	Calculated Model				
	R	R <sub>avg</sub>	R <sub>s</sub>	R <sub>p</sub>	P	$\Delta\phi$ (degrees)
7000	0.851	0.858	0.890	0.825	0.038	147.882
7200	0.849	0.853	0.887	0.819	0.040	148.303
7400	0.844	0.849	0.885	0.813	0.043	148.732
7600	0.839	0.844	0.882	0.806	0.045	149.112
7800	0.833	0.839	0.879	0.799	0.048	149.437
8000	0.825	0.834	0.876	0.792	0.050	149.764
8200	0.821	0.834	0.877	0.792	0.051	150.148
8400	0.822	0.834	0.878	0.791	0.052	150.529
8600	0.823	0.841	0.883	0.798	0.050	150.984
8800	0.831	0.852	0.892	0.812	0.047	151.511
9000	0.849	0.862	0.901	0.824	0.044	152.029
9200	0.867	0.867	0.905	0.830	0.043	152.498
9400	0.881	0.872	0.909	0.836	0.042	152.957
9600	0.893	0.877	0.912	0.841	0.041	153.404
9800	0.903	0.881	0.916	0.846	0.040	153.839
10000	0.910	0.885	0.919	0.851	0.038	154.263

**Figure 5:** Measured and calculated model properties for the HRC M3 mirror.**WFC IM3 Mirror**

The WFC IM3 mirror is placed at a 49.6 degree incidence angle and has a proprietary NIR-enhanced silver coating by Denton Vacuum, Inc. A series of spectrophotometer tracings for witness samples made during coating of this mirror are available (Denton 1997). These are measured at an incidence angle of 45 degrees, which is close to the 49.6 degree

angle for the mirror when mounted in ACS. There are actually slightly different tracings available for two IM3 mirrors. Since it was not known at this time which mirror was actually flown, we have assumed the IM3-1 mirror which had slightly higher (0.2%) reflectivity, and used the tracings for the “IM3-1 witness D1” sample. These tracings show both  $R_s$  and  $R_p$  for the IM3-1 witness and an Aluminum reference mirror. Table 9 gives values read off the tracings. We can then use the Aluminum tracing along with calculated reflectivities for Aluminum (Biretta and McMaster 1997), to calibrate the IM3-1 mirror tracings. Results are given in the four right-hand columns for the s- and r-plane reflectivities as well as the average reflectivity and induced polarization.

**Table 9.** Properties of the WFC IM3 Mirror

Wave length (Å)	Denton Spectrophotometer Plot				Aluminum Model		Corrected / Computed Values			
	IM3-1 Witness		Aluminum Reference							
	$R_s$	$R_p$	$R_s$	$R_p$	$R_s$	$R_p$	$R_s$	$R_p$	$R_{avg}$	P
4000	0.966	0.930	0.939	0.885	0.948	0.899	0.975	0.945	0.960	0.0159
4100	0.978	0.945	0.940	0.888	0.948	0.899	0.986	0.957	0.972	0.0152
4200	0.982	0.951	0.940	0.889	0.948	0.899	0.990	0.962	0.976	0.0147
4400	0.984	0.956	0.940	0.889	0.948	0.898	0.992	0.966	0.979	0.0136
4600	0.980	0.954	0.940	0.888	0.946	0.896	0.986	0.963	0.974	0.0121
4800	0.971	0.950	0.940	0.889	0.945	0.894	0.976	0.955	0.966	0.0108
5000	0.956	0.944	0.940	0.889	0.944	0.891	0.960	0.946	0.953	0.0073
5200	0.943	0.928	0.940	0.881	0.942	0.888	0.945	0.935	0.940	0.0051
5300	0.936	0.928	0.940	0.881	0.941	0.886	0.937	0.933	0.935	0.0020
5400	0.937	0.929	0.940	0.882	0.941	0.885	0.938	0.932	0.935	0.0031
5600	0.945	0.939	0.939	0.882	0.940	0.884	0.946	0.941	0.944	0.0026
5800	0.968	0.950	0.939	0.885	0.939	0.882	0.968	0.947	0.957	0.0111
6000	0.982	0.960	0.941	0.883	0.937	0.878	0.978	0.955	0.966	0.0120
6200	0.983	0.955	0.932	0.869	0.935	0.875	0.986	0.962	0.974	0.0126
6400	0.990	0.961	0.933	0.870	0.934	0.872	0.991	0.963	0.977	0.0143
6600	0.994	0.966	0.933	0.869	0.931	0.866	0.992	0.963	0.977	0.0149
6800	0.997	0.971	0.931	0.866	0.925	0.856	0.991	0.960	0.975	0.0158
7000	1.000	0.975	0.931	0.865	0.920	0.846	0.988	0.954	0.971	0.0178

The Denton spectrophotometer tracing ends at 7000 Angstroms, so some alternate source of information will be needed at longer wavelengths (i.e. for ACS filters F775W and F814W). Woodruff 1996C tabulates  $R_s$  and  $R_p$  from 2500 to 12000 Angstroms for the “Near-IR Optimized Denton Protected Silver Coating” (probably specification values from Denton). These could be used at longer wavelengths, though the Woodruff reflectivities are generally 1% to 2% higher than the spectrophotometer tracing. More importantly, the polarizations in Woodruff are sometimes a factor of 3 or more lower than those derived from the spectrophotometer chart, especially in the far-red. At this time, there is no other information available for the far-red performance.

Unfortunately no lab measurements of the IM3 phase retardance were made. Beckers (1989) indicates the retardance of silver coatings is near 90 degrees for 45 degree incidence angles, which, if correct, implies grave problems for WFC polarimetry. This amount of retardance would convert any incident linear polarization to circular polarization, thus causing a complete loss of information prior to analysis by the linear polarizer filters. The details of the IM3 mirror coating are proprietary, and hence it will be very difficult to reliably calculate the retardance from models. Hueser (1996) has speculated that it might be a three-layer over-coating and has modeled it as 30nm sapphire on silver, an unknown layer about 1000nm thick, and 10nm of  $\text{SiO}_2$ . He derives properties for the middle layer, but the results seem unphysical as the predicted middle layer refractive index varies wildly with wavelength. Private discussions with Hartig suggest possibly a three-layer  $\text{MgF}_2$  coating, with cleaning between layers to avoid pinholes through to the silver layer. However, we have run several coating models based on silver /  $\text{MgF}_2$ , and there is poor agreement with the measured reflectivities of the mirror. At this time there is not enough information available to reliably compute the phase retardance.

Given the lack of information, we have run several models merely to get a rough idea of what retardance values are possible for silver coatings. For a bare silver surface at the appropriate incidence angle, we find phase retardance values between 144 and 161 degrees, between 4800 and 7800 Angstroms, respectively. We have also tried single-layer coatings of  $\text{MgF}_2$ ,  $\text{SiO}_2$ , and  $\text{HfO}_2$ . These produce phase retardances in the range 150 to 176 degrees for thicknesses giving high-reflectivity. This argues against the large retardance effects suggested by the Beckers (1989) result, but the applicability of these models is difficult to judge without more information on the coating.

### ***CCD Detectors***

Most astronomical cameras utilize CCDs at near-normal incidence angles, and simple symmetry arguments thus ensure the absence of significant polarization effects. ACS,

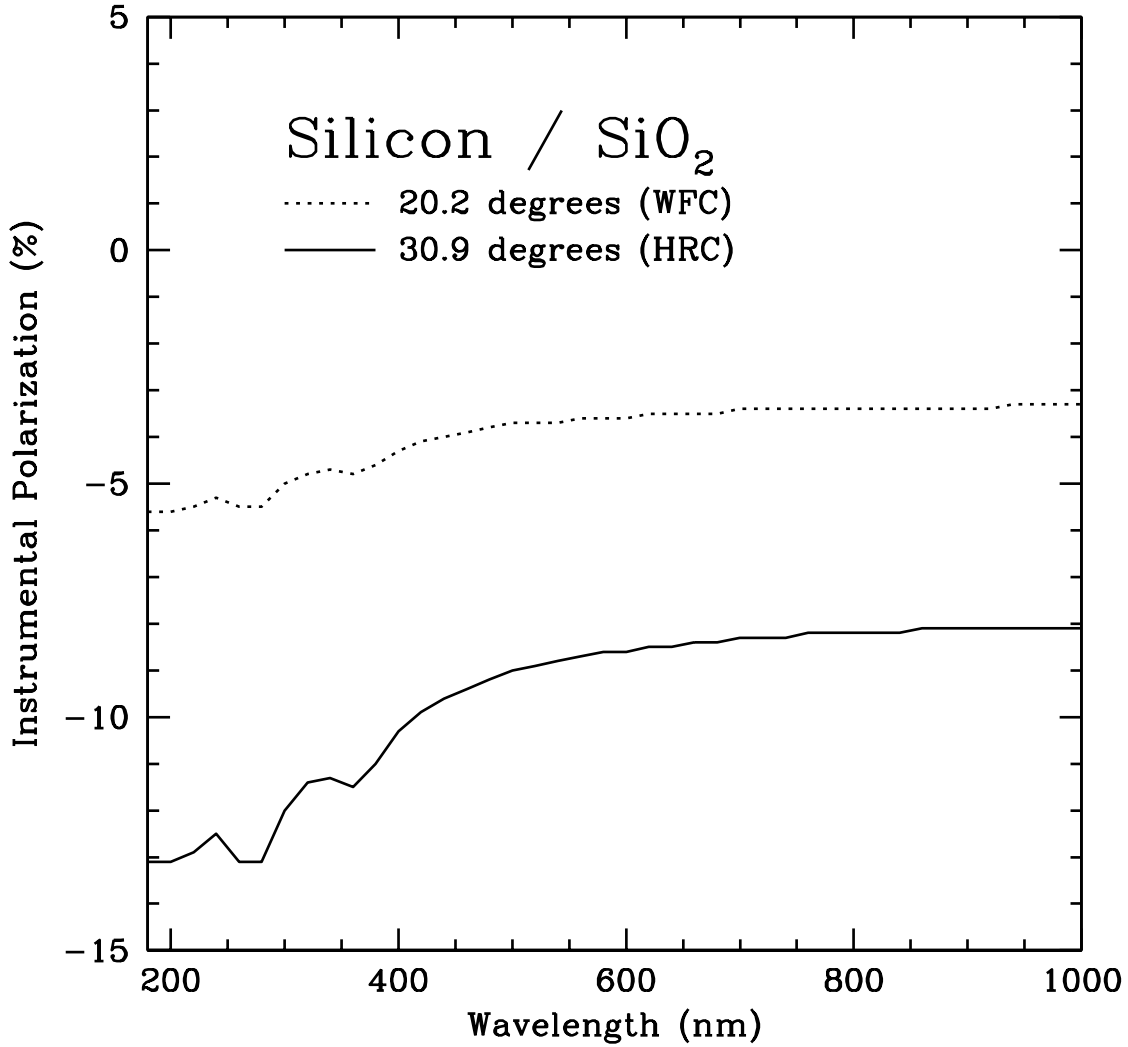
however, utilizes CCD detectors at large tilts as required by its optical prescription. This has the potential to introduce large polarization effects. We are unaware of any pre-launch measurements of the polarization properties of the ACS CCDs<sup>1</sup>; lacking such information we can only attempt to estimate the size of the potential polarization effects. The details of the CCD surfaces and their coatings are presently unknown<sup>2</sup>, which will prevent an accurate model. Here we simply model the CCDs as a Silicon surface with a 1 Angstrom thick SiO<sub>2</sub> layer. Figure 6 shows the resulting polarizations for the transmission of light into the silicon surface computed with the equations described by Biretta and McMaster 1997. The incidence angle of 20.2 degrees represents the WFC CCD, and the 30.9 degree angle represents the HRC CCD. Clearly there is a potential for large polarization effects -- the largest values appear to be in the UV and reach about 13% for the HRC. Effects for the WFC are around 3% to 4% at visible wavelengths. The polarizations are

---

1. Private communications with M. Clampin and G. Hartig.  
2. Both the HRC and WFC CCDs were coated by SITE and the details are thought to be proprietary. M. Lesser has suggested the coating is probably ~15 nm of HfO<sub>2</sub>.

negative as a matter of sign convention; here the intensity of the  $T_M$  mode (or p-mode) is greater than the  $T_E$  mode (or s-mode).

**Figure 6:** Polarization for transmission into tilted Silicon surfaces.



#### ***RAS/HOMS Test at Ball -- 2001 March 2***

After integration of ACS, the instrumental polarization was measured using the RAS/HOMS<sup>1</sup> fed by a white light fiber optic illuminator with a QTH lamp. In addition, a mylar diffuser was placed at the RAS pupil plane to simulate a OTA illumination over the entire field of view. Flat fields were obtained in several spectral filters together with each of the

---

1. Refractive Aberrated Simulator / Hubble Opto-Mechanical Simulator

three polarizers in each set. The resulting counts in the flats were used to derive the instrumental polarization, and these are given in Table 10 (from [http://acs.pha.jhu.edu/instrument/calibration/results/by\\_item/polarimetry/instpol\\_test](http://acs.pha.jhu.edu/instrument/calibration/results/by_item/polarimetry/instpol_test)).

**Table 10.** Instrumental Polarization (pre-launch).

Camera	Pol. Filter Set	Spectral Filter	P(%)
HRC	POLUV	F435W	4.5
		F814W	3.6
	POLV	F555W	3.7
		F775W	1.2
WFC	POLUV	F435W	2.7
		F814W	0.6
	POLV	F555W	6.0
		F775W	5.1

Unfortunately the RAS/HOMS optics are likely to have considerable polarization themselves. It was originally designed to test COSTAR, where polarization was not a concern. Besides the six lenses there are two mirrors at 45 degree incidence angles which are used to turn the light beam through 180 degrees. For standard aluminum coatings with silicon oxide over-coats each mirror would contribute about 3% polarization (6000 Angstroms), for a total of 6% polarization -- thus thoroughly corrupting the ACS polarization measurement. The mylar diffusing screen probably helped somewhat to reduce the RAS/HOMS polarization, but assuming light passed through the screen with only one or two scatterings, there was probably only a modest reduction in the RAS/HOMS polarization.<sup>1</sup>

### *RAS/Cal Test at GSFC -- 2001 August 15-22*

An effort was made to measure the angles of the polarizer filters in the assembled ACS using the RAS/Cal<sup>2</sup> facility at GSFC. A Glan-Thompson polarizing prism was mounted on a precision rotating stage and placed in the RAS/Cal beam directly in front of the ACS entrance aperture. The broad-band QTH lamp was used as a light source. The brightness in the ACS images was then measured as a function of the rotating stage angle. Measure-

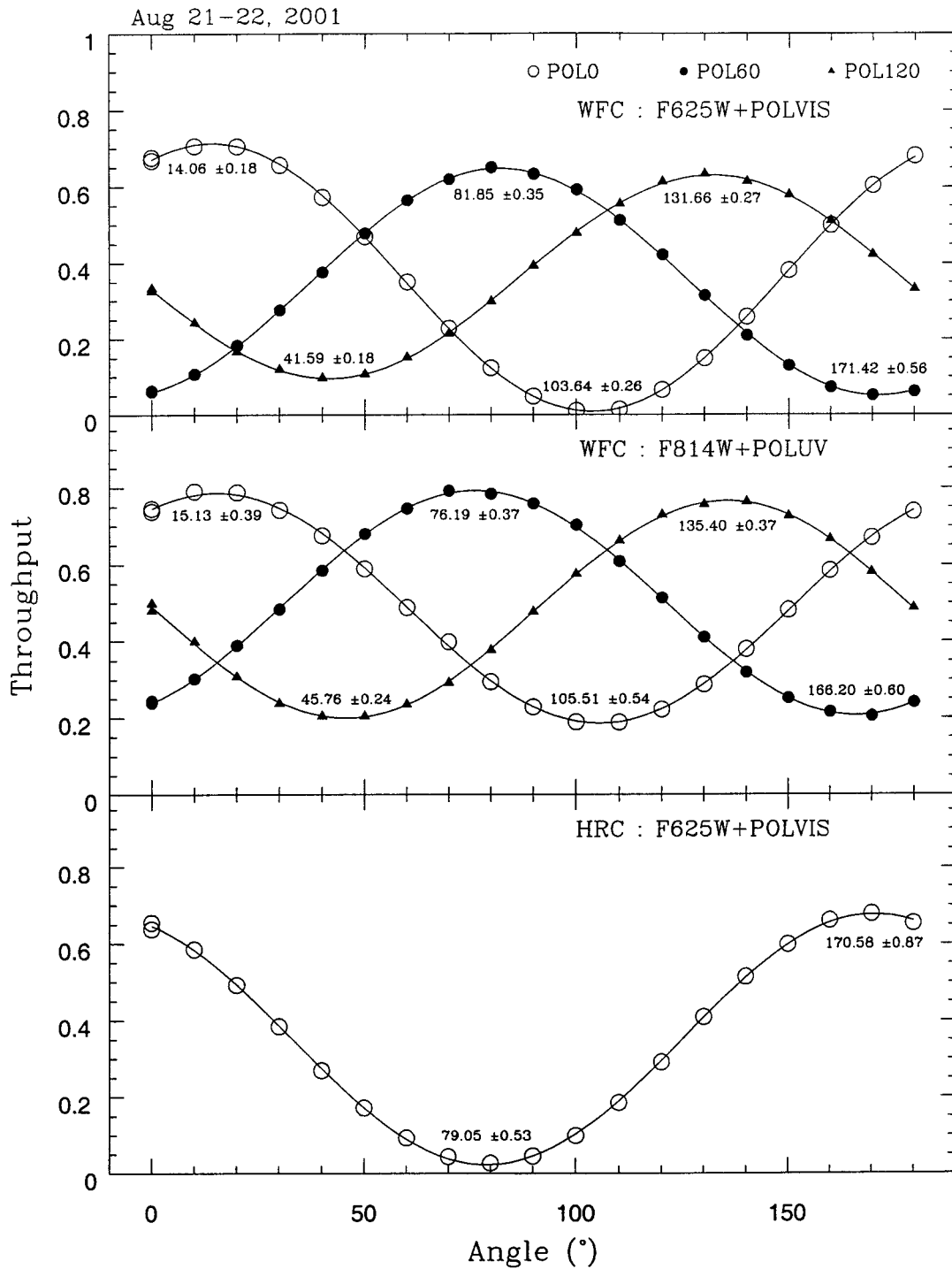
---

1. The ACS ground test plan describes a second more accurate set of measurements of instrumental polarization to be performed at GSFC with a Spectralon reflective diffuser; however these tests were never actually conducted.

2. Reflective Aberrated Simulator / Calibrator

ments in several filters at multiple field positions were planned for both cameras. However a serious problem was discovered on August 21 which invalidated all the prior data -- apparently part of the apparatus used for previous tests did not move fully when commanded out of the beam, and remained partially in the RAS/Cal optical beam during the polarization measurements (Hartig and Martel 2001). A limited set of good measurements were obtained on 21 and 22 August, and these are shown in Figure 7 (Martel 2003).

**Figure 7:** Results from RAS/Cal polarizer angle test 21-22 August 2001<sup>1</sup>.



These plots give the ACS countrate (normalized relative to the rate with no ACS polarizer filter in the beam), as a function of the angle on the external rotating stage. For the WFC a

1. From Martel 2003.

400x400 pixel subimage was used at amplifier B pixel 760,2750; for HRC a similar subimage was used at amplifier C pixel 480,330. Curves were then fit to the data, resulting in the interpolated angles on the rotating stage for maximum and minimum countrates given in Table 11.

**Table 11.** Polarizer Angles from August 2001 RAS/Cal Pre-Launch Test

Camera	Spectral Filter	Polarizer	Intensity	Measured Angle on Rotating Stage (degrees)	Computed Angle on Sky CCW from +V3 (degrees)
HRC	F625W	POL0V	Maximum	170.58±0.87	117.02±0.87
			Minimum	79.05±0.53	25.50±0.53
WFC	F625W	POL0V	Maximum	14.06±0.18	-39.49±0.18
			Minimum	103.64±0.26	50.09±0.26
		POL60V	Maximum	81.85±0.35	28.30±0.35
			Minimum	171.42±0.56	117.87±0.56
		POL120V	Maximum	131.66±0.27	78.11±0.27
			Minimum	41.59±0.18	-11.96±0.18
WFC	F814W	POL0UV	Maximum	15.13±0.39	-38.42±0.39
			Minimum	105.51±0.54	51.96±0.54
		POL60UV	Maximum	76.19±0.37	22.64±0.37
			Minimum	166.20±0.60	112.65±0.60
		POL120UV	Maximum	135.40±0.37	81.85±0.37
			Minimum	45.76±0.24	-7.79±0.24

We ultimately want to know the polarizer angles on the sky in the usual (V3,V2) system; these may be calculated from the rotating stage angles as follows. The rotating stage assembly contained an optical cube on the non-rotating part which served as an angle reference. On 7 August 2001 the polarizer/rotating stage assembly was calibrated separately relative to the optical cube; the polarizer E-field vector was found to be parallel to the optical cube normal when the rotating stage angle read 7.9548 degrees (Kubalak 2001). Clockwise rotation of the polarizer corresponded to increasing angle readout on the rotating stage (clockwise when viewing into the STOPT +Z direction). On 21 August 2001, during the measurements on the ACS polarizer filters, the rotating stage assembly was cal-

ibrated relative to the STOPT reference frame. It was found that the optical cube normal was rotated 0.6033 degrees counter-clockwise from STOPT -X axis (viewing into the +Z direction or equivalently into the ACS entrance aperture). Finally, the STOPT -X direction is nominally 45 degrees counter-clockwise from the +V3 direction (again viewing into the +Z direction). Using this information the polarizer angles measured on the rotating stage can be converted to angles relative to the spacecraft +V3 direction. A sample calculation is shown in Table 12, where counter-clockwise angles on the sky are given (viewing into the

**Table 12.** Sample Calculation of Polarizer V3 Angle (HRC POL0V + F625W)

Measurement	Angle (degrees CCW looking at sky or STOPT -Z direction)
Rotating stage readout at maximum transmission	170.58
Optical cube normal rotation relative to rotating stage zero point	-(7.9548)
STOPT -X axis rotation relative to the optical cube normal	-(0.6033)
+V3 axis rotation relative to STOPT -X axis	-(45)
Result (sum): HRC POL0V+F625W relative to +V3 axis	117.02

STOPT -Z direction) for the HRC POL0V+ F625W data; results for other camera/filter combinations are given in the right-most column of Table 11. In short, the angles relative to the +V3 axis can be computed by subtracting 53.56 degrees from the rotating stage angles. The accuracy of the computed angles relative to the +V3 axis is probably limited mostly by the interpolation of the rotating stage measurement, and by the accuracy of the nominal 45 degree angle between the +V3 and STOPT -X axes. The measured angles from the STOPT -X axis to the optical cube normal, and from there to the rotating stage zero, appear to be measured to very high precision.

Later in Section 7 on page 53 we will compare these polarizer angles derived from the RAS/Cal test (Table 12) with those derived from the design specifications (Table 5, 6, 7).

It is interesting to compare the angles measured for the different polarizer filters. While there might be some error in calibrating the external rotating stage, the *relative* angles should remain accurate. In the simplest scenario, we might expect the angles for the 0, 60, and 120 degree polarizers to differ by their nominal 60 degree rotations. The angle differ-

ences are shown in Table 13. As can be seen, the F625W + POLV results show significant

**Table 13.** Relative Polarizer Angles from August 2001 RAS/Cal Test

Camera	Spectral Filter	Polarizer	Intensity	Rotation from POL0 (degrees)
WFC	F625W	POL60V	Maximum	67.8±0.6
			Minimum	67.8±0.9
		POL120V	Maximum	117.6±0.7
			Minimum	118.0±0.8
WFC	F814W	POL60UV	Maximum	61.1±0.8
			Minimum	60.7±1.1
		POL120UV	Maximum	120.3±0.9
			Minimum	120.2±0.7

deviations from the expected rotation angles. For example, while the nominal rotation between POL0V and POL60V is 60 degrees, the measured value for WFC with F625W is 67.8 degrees, thus giving an apparent anomaly of  $7.8 \pm 0.6$  degrees. The data for POL120V also show an anomaly of  $\sim 2$  degrees. In contrast, the results for F814W with the UV polarizers are within the uncertainties of the expected rotations.

There are several possible explanations for these anomalous POLV filter rotations. Spurious polarization effects in either ACS and/or RAS/Cal appear to be one likely cause. It is interesting to note that the minimum and maximum *throughputs* for WFC with F625W+POLV in Figure 7 also show extremely anomalous behavior. If the three POLV filters were identical in their properties, as is thought to be the case, we should expect identical tracings for the three filters in the top panel of Figure 7, except for the nominal 60 degree shifts. However, it is readily apparent that the throughputs at the minima and maxima of the curves are quite different among the three filters. The POL0V filter shows a minimum transmission around 1% while that of the POL120V filter is about 10%, and POL60V is somewhere in between. Similarly the maxima for POL0V is about 81% while that for POL120V is 63%. This type of behavior is a fairly clear sign of spurious polarization. We have made simulations of the RAS/Cal + ACS system using the Mueller matrix methodology of Biretta and McMaster 1997, and both the anomalous angles and maximum throughputs for POLV can be reproduced by a 13% spurious polarization somewhere in the optics, however other details like the angles of minimum throughput are not reproduced very well. Detailed modeling of the RAS/Cal optics<sup>1</sup> suggest it should not

contribute more than a few percent polarization. Also, it would be difficult to explain why the F814W + POLUV results agreed well with expectations if the problem were in RAS/Cal, as we do not expect strong wavelength effects in RAS/Cal.

It seems one must instead turn to anomalies in the ACS optics to find the cause of the angle anomalies. At this point we see four possibilities:

1. One or more of the POLV filters are mounted in the filter wheel at the wrong angle. But nearly 8 degrees of error is surprising. Any reasonable amount of care in mounting the filters should result in angles accurate to a small fraction of a degree. (As we will discuss later, comparison of the RAS/Cal data with the design spec angles also argues against this possibility.)
2. The F625W filter is somehow anomalous, possessing either internal polarization or birefringence.
3. There is a large and unexpected source of polarization within the WFC with a very strong wavelength dependence. Such an anomaly would need to impact F625W but not F814W. The measured polarization of the IM3 mirror is only a few percent (Table 9), so it seems an unlikely cause, unless of course it has large phase retardance effects. Effects within the WFC CCD are another potential cause.
4. There is some measurement error which impacts only the WFC F625W + POLV data.

In summary, this test gave anomalous angles and throughputs for the POLV filters with the F625W filter. This could be caused by spurious polarization effects in ACS, or rather less likely, within RAS/Cal. For the POLUV filters with F814W the angles were within errors of the nominal 60 degree rotations, and the throughputs exhibited much more normal behavior.

---

1. There are eight mirrors in the RAS/Cal system, though most of these operate at near-normal incidence angles. The coatings are reputed to be a UV-optimized  $\text{MgF}_2$  over-coated aluminum. Two mirrors are used at 45 degree incidence angles to steer the beam into ACS; however their axes are at  $\sim 90$  degrees to each other, so the polarization effects should nearly cancel. We estimate that even with a few degrees of misalignment from the 90 degree angle, these mirrors should produce less than 0.5% polarization. There are four mirrors used at  $\sim 15$  degree incidence angle with axes parallel, and we estimate these would contribute 1% or less polarization. It is also possible that the lamp system contributes polarization, but it contains only axial optics, and hence should have little or no polarization effects. Some discussions indicated a mylar diffusing screen was used between RAS/Cal and the polarizing rotating stage to eliminate spurious polarization, but the current understanding is that the diffuser was not actually used for the RAS/Cal test. Unless the lamp system was highly polarized, it seems difficult to produce enough spurious polarization in RAS/Cal to account for the 13% spurious polarization needed to explain the POLV + F625W results.

## 6. On-Orbit Calibrations

There are currently three programs which have taken on-orbit calibrations for the polarizers. As of this writing the first two, 9586 and 9661 have completed, and 10055 is still underway. We now describe these programs in detail and present early results where they are available.

### Proposal 9586 “ACS Polarization Calibration”

Proposal 9586 (Sparks PI) was designed to perform the initial on-orbit calibration of the ACS polarizers. Here we review the motivation and observing plan of this proposal on a visit-by-visit basis. Some discussion of the initial assessment of the data quality is included here, as well as preliminary photometry for the standard stars, but more detailed analyses are deferred until later. Table 16 gives details of the individual exposures. The program totals 25 orbits.

#### *Visit 1: WFC, polarized star Vela, 2 orbits.*

This visit observes a polarized standard star in the WFC in three commonly used spectral filters (F475W, F606W, and F775W) crossed with the three POL\_V filters. The purpose of these data are to assess the instrumental polarization, and measure errors in the derived polarization position angles (goals 1, 2 and 4 on page 5 and page 6) for the WFC. The target has been calibrated from the ground by Whittet, et al., 1992 (Vela I No. 81), who give the polarizations listed in Table 14. It turns out this object is a double star with 1” separation and magnitude difference  $\sim 2$  mag, which will lead to some complications in performing aperture photometry. Several of the F475W and F775W images were saturated.

**Table 14.** Vela I No. 81 Ground Photometry

Band	$p$ (%)	$\sigma(p)$	$PA$	$\sigma(PA)$
U	5.0	0.6	1	3
B	6.1	0.3	1	1
V	6.86	0.13	1	3
R	6.85	0.19	1	1
I	6.29	0.10	179	1

**Visit 2: WFC, unpolarized star GD319, 2 orbits.**

This visit observes an unpolarized standard star in the WFC in three commonly used spectral filters (F475W, F606W, and F775W) crossed with the three POL\_V filters. The purpose of these data are primarily to assess the instrumental polarization (goals 1 and 2 on page 5 and page 6). In effect these data are the corner stone of the polarization calibration for the WFC. Ideally the unpolarized target should produce identical signals in all three POLnV filters (n=0, 60, 120 degrees), and hence differences in the signals are a strong discriminant of instrumental polarization. In principle, these data could also be used to estimate the polarizer throughputs (goal #3 on page 6), though no images were taken of this star without the polarizers in place.

This target has been calibrated from the ground by Schmidt, Elston, and Lupie (1992). They give polarizations of  $0.065 \pm 0.033$  ,  $0.045 \pm 0.047$  , and  $0.089 \pm 0.093$  percent at U, B, and V bands, respectively. From our data, it is apparent that this is a double star with  $\sim 2.5''$  separation and strongly differing colors (magnitude difference 1.3 mag in F475W, but 0.1 mag in F775W). This raises some concerns about the ground-based photometry; the smallest aperture on the instrument used by Schmidt, Elston, and Lupie (“Two-Holer”) is  $4.2''$  in diameter, though it is believed the  $8''$  aperture was used; in either case it seems likely that some (but perhaps not all) light from the fainter star was recorded during ground calibrations. For the purpose of identification we designate the blue star as “A” (top star in WFC images, at pixel  $x=1051.9$  and  $y=1056.9$  in the observed subarray), and the redder star as “B.”

**Visit 3: HRC, polarized star BD+64DEG106, 3 orbits.**

This visit observes a polarized standard star in the HRC in many commonly used spectral filters. Specifically F475W, F606W, F625W, F658W, and F775W are crossed with the three POL\_V filters. And F220W, F250W, F330W, F435W, and F814W are crossed with the three POL\_UV filters. The goals are similar to Visit 1, that is to assess the instrumental polarization, and measure errors in the derived polarization position angles, but here for the HRC. The target has been calibrated from the ground by Schmidt, Elston, and Lupie (1992) with results given in Table 15.

**Table 15.** BD+64deg106 Ground Photometry

Band	$p$ (%)	$\sigma(p)$	$PA$	$\sigma(PA)$
U	5.110	0.104	97.04	0.58
B	5.506	0.090	97.15	0.47
V	5.687	0.037	96.63	0.18

**Table 15.** BD+64deg106 Ground Photometry

Band	$p$ (%)	$\sigma(p)$	$PA$	$\sigma(PA)$
R	5.150	0.098	96.74	0.54
I	4.696	0.052	96.89	0.32

***Visit 4: HRC, unpolarized star GD319, 5 orbits.***

This visit observes an unpolarized standard star in the HRC in many commonly used spectral filters. Specifically F475W, F606W, F625W, F658W, and F775W are crossed with the three POL\_V filters. And F220W, F250W, F330W, F435W, and F814W are crossed with the three POL\_UV filters. The purpose of these data are primarily to assess the instrumental polarization. In effect these data are the corner stone of the polarization calibration for the HRC. Again, the unpolarized target should produce identical signals in all three POLnV (or POLnUV) filters ( $n=0, 60, 120$  degrees), and hence differences in the signals are a strong discriminant of instrumental polarization. In principle, these data could also be used to estimate the polarizer throughputs, though no images were taken without the polarizers in place. See Visit 2 notes for details about the target. This object is a double star with  $\sim 2.5''$  separation and strongly differing colors; this has led to saturation of the F220W, F250W, and F330W images for the bluer star of the pair, which will complicate aperture photometry. For the purpose of identification we designate the blue star as "A" (bottom star in HRC images, at pixel  $x=644$  and  $y=594$ ), and the redder star as "B."

***Visit 5: WFC, polarized diffuse target CRL2688-2, 2 orbits.***

This visit observes a polarized diffuse nebula in the WFC in F606W crossed with the three POL\_V filters. The purpose of these data are to test our ability to make an ACS polarization image of an extended target. In addition, comparison of that image with ground data will allow assessment of the polarizer flat field accuracy and any adverse photometry impact due to the geometric correction (goals 5 and 7 on page 6). Unfortunately bad target coords were used and all data were lost.

***Visit 6: HRC, polarized diffuse target CRL2688-2, 1 orbit.***

This visit observes a polarized diffuse nebula in the WFC in F606W crossed with the three POL\_V filters. The purpose of these data are to test our ability to make an ACS polarization image of an extended target with HRC. In addition, comparison of that image with ground data will allow assessment of the polarizer flat field accuracy and any adverse photometry impact due to the geometric correction (same goals as Visit 5). Unfortunately bad target coords were used and all data were lost.

***Visit 7: HRC, core of star cluster NGC104 (47 Tuc), 3 orbits.***

This visit observes a weakly polarized star cluster with the HRC for a few representative filters -- F220W, F330W, and F435W are crossed with the three POL\_UV filters. And F475W, F606W, and F658N are crossed with the three POL\_V filters. The purpose of these data are to test the accuracy of the polarization calibration across the HRC field-of-view, and to measure the geometric distortion contributed by optical power in the polarizer filters (goals 5, 6, and 7 on page 6). The F658N filter is included since it is thought to give a different filter-filter reflection pattern than the other filters, and hence will be useful in assessing errors caused by reflections in the flat fields. The polarization properties of the target are discussed by Forte, et al., 2002.

***Visit 8: WFC, outer region of star cluster NGC104-OUTER (47 Tuc), 3 orbits.***

This visit observes a weakly polarized star cluster with the WFC for a few representative filters -- F475W, F606W, and F658N are crossed with the three POL\_V filters. The purpose of these data are to test the accuracy of the polarization calibration across the WFC field-of-view, and to measure the geometric distortion contributed by optical power in the polarizer filters (same goals as Visit 7). The F658N filter is included since it is thought to give a different filter-filter reflection pattern than the other filters, and hence will be useful in assessing errors due to reflections in the flat fields. The polarization properties of the target are discussed by Forte, et al., 2002.

***Visit 55: WFC, polarized diffuse target CRL2688-2, 3 orbits.***

This visit observes a polarized diffuse nebula in the WFC in F606W crossed with the three POL\_V filters. The purpose of these data are to test our ability to make an ACS polarization image of an extended target. In addition, comparison of that image with ground data will allow assessment of the polarizer flat field accuracy and any adverse photometry impact due to the geometric correction (goals 5 and 7 on page 6). This repeats Visit 5 with corrected target coords.

***Visit 56: HRC, polarized diffuse target CRL2688-2, 1 orbit.***

This visit observes a polarized diffuse nebula in the WFC in F606W crossed with the three POL\_V filters. The purpose of these data are to test our ability to make an ACS polarization image of an extended target with HRC. In addition, comparison of that image with ground data will allow assessment of the polarizer flat field accuracy and any adverse photometry impact due to the geometric correction (same goals as Visit 55). This repeats Visit 6 with corrected target coords.

**List of Exposures**

Table 16 below lists the exposures in program 9586. For each visit, the first row gives the visit number, the detector (HRC or WFC), the target, observation date, and PA\_V3. The remaining rows for each visit give information for the individual images including the image name, filters, exposure time, and the resulting count rate for each star. Image names refer to the \_drz.fits file. Exposure times are the total for all the CR-SPLITS. Count rates are for the combined drizzled image and are in units of detected electrons per second. Several of the stars are double stars, and in these situations we give count rates for both stars of the pair, formatted as star A / star B. In some cases an image is saturated and the measured counts are suspect; these are indicated by (). See *note added in proof* on page 62.

**Table 16.** Summary of exposures for proposal 9586

Visit	Detector	Target	Date	PA_V3 (deg)	Notes
Images	Filter1	Filter2	Exp. Time (s)	Count Rate (e- / s) (Star A / B)	
Visit 1	WFC	Vela	5/25/2002	296.3	
j8gh01011	F475W	POL0V	39	18952 / 3457	
j8gh01021	F475W	POL60V	39	19244 / 3593	Star A saturated <sup>a</sup>
j8gh01031	F475W	POL120V	39	20687 / 3834	Star A saturated <sup>a</sup>
j8gh01041	F606W	POL0V	9	60797 / 12313	
j8gh01051	F606W	POL60V	9	63247 / 12900	
j8gh01061	F606W	POL120V	9	68474 / 13791	
j8gh01071	F775W	POL0V	9	73590 / 16694	
j8gh01081	F775W	POL60V	9	75041 / 17011	
j8gh01091	F775W	POL120V	9	77887 / 18048	Star A saturated <sup>a</sup>
Visit 2	WFC	GD319	5/28/2002	312.6	
j8gh02011	F475W	POL0V	9	90813 / 23845	
j8gh02021	F475W	POL60V	9	88198 / 23263	
j8gh02031	F475W	POL120V	9	90809 / 23959	
j8gh02041	F606W	POL0V	6	103102 / 66723	
j8gh02051	F606W	POL60V	6	101074 / 65260	
j8gh02061	F606W	POL120V	6	104447 / 67694	
j8gh02071	F775W	POL0V	12	37019 / 58118	

**Table 16.** Summary of exposures for proposal 9586

Visit	Detector	Target	Date	PA_V3 (deg)	Notes
Images	Filter1	Filter2	Exp. Time (s)	Count Rate (e- / s) (Star A / B)	
j8gh02081	F775W	POL60V	12	36097 / 56799	
j8gh02091	F775W	POL120V	12	36670 / 57606	
Visit 3	HRC	BD+64D106	6/25/2002	88.5	
j8gh03011	F475W	POL0V	6	259951	
j8gh03021	F475W	POL60V	6	310140	
j8gh03031	F475W	POL120V	6	309473	
j8gh03041	F606W	POL0V	2	607846	
j8gh03051	F606W	POL60V	2	723703	
j8gh03061	F606W	POL120V	2	709541	
j8gh03071	F625W	POL0V	4	386375	
j8gh03081	F625W	POL60V	4	447779	
j8gh030a1	F625W	POL120V	4	435421	
j8gh030b1	F658N	POL0V	70	21494	
j8gh030c1	F658N	POL60V	70	25795	
j8gh030d1	F658N	POL120V	70	25196	
j8gh030g1	F775W	POL0V	4	408886	
j8gh030f1	F775W	POL60V	4	468148	
j8gh030e1	F775W	POL120V	4	444175	
j8gh03091	POL0UV	F220W	1040	381	
j8gh030h1	POL60UV	F220W	1040	456	
j8gh030o1	POL120UV	F220W	1040	383	
j8gh030s1	POL0UV	F250W	200	4066	
j8gh030t1	POL60UV	F250W	200	4846	
j8gh030u1	POL120UV	F250W	200	4242	
j8gh030p1	POL0UV	F330W	35	19962	
j8gh030q1	POL60UV	F330W	35	24281	
j8gh030r1	POL120UV	F330W	35	22165	
j8gh030l1	POL0UV	F435W	9	125184	
j8gh030m1	POL60UV	F435W	9	157388	

**Table 16.** Summary of exposures for proposal 9586

Visit	Detector	Target	Date	PA_V3 (deg)	Notes
Images	Filter1	Filter2	Exp. Time (s)	Count Rate (e- / s) (Star A / B)	
j8gh030n1	POL120UV	F435W	9	145953	
j8gh030i1	POL0UV	F814W	4	682511	
j8gh030j1	POL60UV	F814W	4	756203	
j8gh030k1	POL120UV	F814W	4	711585	
Visit 4	HRC	GD319	5/21/2002	317.5	
j8gh04041	F475W	POL0V	24	49901 / 13692	
j8gh04051	F475W	POL60V	24	54619 / 14890	
j8gh04061	F475W	POL120V	24	56316 / 15326	
j8gh04011	F606W	POL0V	18	58906 / 38042	
j8gh04021	F606W	POL60V	18	64230 / 41333	
j8gh04031	F606W	POL120V	18	65150 / 41870	
j8gh04071	F625W	POL0V	36	29056 / 25464	
j8gh04081	F625W	POL60V	36	31017 / 27156	
j8gh040a1	F625W	POL120V	36	31051 / 27068	
j8gh04091	F658N	POL0V	810	1313 / 1467	
j8gh040e1	F658N	POL60V	810	1436 / 1604	
j8gh040f1	F658N	POL120V	810	1436 / 1597	
j8gh040b1	F775W	POL0V	51	17292 / 27166	
j8gh040c1	F775W	POL60V	51	18596 / 29186	
j8gh040d1	F775W	POL120V	51	18060 / 28306	
j8gh040t1	POL0UV	F220W	800	(3735) / 4.7	Star A sat 2pix <sup>b</sup>
j8gh040s1	POL60UV	F220W	800	(4304) / 1.5	Star A sat 4pix <sup>b</sup>
j8gh040u1	POL120UV	F220W	800	(3450) / 1.8	Star A sat 4pix <sup>b</sup>
j8gh040o1	POL0UV	F250W	570	(9873) / 23.0	Star A sat 8pix <sup>b</sup>
j8gh040p1	POL60UV	F250W	570	(10944) / 26.0	Star A sat 9pix <sup>b</sup>
j8gh040q1	POL120UV	F250W	570	(9617) / 23.8	Star A sat 9pix <sup>b</sup>
j8gh040r1	POL0UV	F330W	225	(16757) / 323	Star A sat 3pix <sup>b</sup>
j8gh040g1	POL60UV	F330W	225	(18856) / 372	Star A sat 6pix <sup>b</sup>

**Table 16.** Summary of exposures for proposal 9586

Visit	Detector	Target	Date	PA_V3 (deg)	Notes
Images	Filter1	Filter2	Exp. Time (s)	Count Rate (e- / s) (Star A / B)	
j8gh040h1	POL120UV	F330W	225	(17589) / 351	Star A sat 5pix <sup>b</sup>
j8gh040i1	POL0UV	F435W	30	35840 / 5364	
j8gh040m1	POL60UV	F435W	30	41577 / 6266	
j8gh040n1	POL120UV	F435W	30	39683 / 5968	
j8gh040o1	POL0UV	F814W	45	24618 / 44129	
j8gh040j1	POL60UV	F814W	45	26720 / 47686	
j8gh040k1	POL120UV	F814W	45	25254 / 45265	
Visit 5	WFC	CRL2688-2	6/1/2002		
j8gh050i1	F606W	POL0V	999	N/A	Bad coords
j8gh050j1	F606W	POL60V	999		Bad coords
j8gh050k1	F606W	POL120V	999		Bad coords
Visit 6	HRC	CRL2688-2	6/1/2002		
j8gh060i1	F606W	POL0V	750	N/A	Bad coords
j8gh060j1	F606W	POL60V	750		Bad coords
j8gh060k1	F606W	POL120V	750		Bad coords
Visit 7	HRC	NGC104	5/28/2002	55.3	
j8gh070i1	POL0UV	F220W	600	TBD	
j8gh070j1	POL60UV	F220W	600		
j8gh070k1	POL120UV	F220W	600		
j8gh070l1	POL0UV	F330W	300	TBD	
j8gh070m1	POL60UV	F330W	300		
j8gh070n1	POL120UV	F330W	300		
j8gh070o1	POL0UV	F435W	120	TBD	
j8gh070p1	POL60UV	F435W	120		
j8gh070q1	POL120UV	F435W	120		
j8gh070a1	F475W	POL0V	600	TBD	Saturated 10+ pix <sup>c</sup>
j8gh070b1	F475W	POL60V	600		Saturated 10+ pix <sup>c</sup>
j8gh070c1	F475W	POL120V	600		Saturated 10+ pix <sup>c</sup>

**Table 16.** Summary of exposures for proposal 9586

Visit	Detector	Target	Date	PA_V3 (deg)	Notes
Images	Filter1	Filter2	Exp. Time (s)	Count Rate (e- / s) (Star A / B)	
j8gh070d1	F606W	POL0V	300	TBD	Saturated 10+ pix <sup>c</sup>
j8gh070e1	F606W	POL60V	300		Saturated 10+ pix <sup>c</sup>
j8gh070f1	F606W	POL120V	300		Saturated 10+ pix <sup>c</sup>
j8gh070g1	F658N	POL0V	120	TBD	
j8gh070h1	F658N	POL60V	120		
j8gh070i1	F658N	POL120V	120		
Visit 8	WFC	NGC104- OUTER	5/25/2002	52.1	
j8gh08011	F475W	POL0V	120	TBD	Saturated 5 pix <sup>c</sup>
j8gh08021	F475W	POL60V	120		Saturated 5 pix <sup>c</sup>
j8gh08031	F475W	POL120V	120		Saturated 7 pix <sup>c</sup>
j8gh08041	F606W	POL0V	120	TBD	
j8gh08051	F606W	POL60V	120		
j8gh08061	F606W	POL120V	120		
j8gh08071	F658N	POL0V	120	TBD	
j8gh08081	F658N	POL60V	120		
j8gh08091	F658N	POL120V	120		
Visit 55	WFC	CRL2688-2	10/15/2002	278.0	
j8gh55011	F606W	POL0V	999	TBD	Some saturation <sup>d</sup>
j8gh55021	F606W	POL60V	999		Some saturation <sup>d</sup>
j8gh55031	F606W	POL120V	999		Some saturation <sup>d</sup>
j8gh55plq	F606W	CLEAR2L	110	TBD	Some saturation <sup>d</sup>
j8gh55pnq	F606W	CLEAR2L	360		Strong saturation <sup>d</sup>
Visit 56	HRC	CRL2688-2	9/27/2002	296.8	
j8gh56011	F606W	POL0V	750	TBD	
j8gh56021	F606W	POL60V	750		
j8gh56031	F606W	POL120V	750		

a. A-to-D converter saturated.

- b. In several of the images one star of the pair is saturated due to a combination of a-to-d converter over-run and exceeding the CCD full well. These count rates are indicated by (). Since the CCD full well is only slightly greater than the a-to-d converter limit (e.g. 155000 electrons vs. 130000 electrons for HRC with default GAIN=2), these values are still probably good to 10% to 15% -- not good enough for polarimetry, but adequate for estimating future exposures on these stars. Somewhat greater accuracy can probably be obtained by multiplying the number of saturated pixels (in last column) by the difference between the CCD full well and a-to-d converter limit (about 25000 electrons per saturated pixel for HRC), and correcting the counts upwards by this amount.
- c. The brightest stars in cluster are saturated over 5 or more pixels, but fainter stars should be OK.
- d. Bright regions of the nebula are saturated; fainter regions may be usable.

### ***Preliminary Analyses and Results for 9586***

Here we discuss only reductions for the standard star data, which should be relatively straight-forward; analyses of other data are left for future reports. Reduction of the data for the standard stars GD319, Vela I, and BD+64D106 were performed using the pipeline drizzled images (`_drz.fits` files). For the HRC images a 20 pixel radius aperture was used centered on the star, and the sky was determined using an annulus centered on the star with inner and outer radii of 20 and 40 pixels, respectively. For the WFC a 10 pixel radius aperture was used on the star, and the sky region had inner and outer radii of 10 and 20 pixels, respectively. Two of the stars are double which presents potential complications for the sky subtraction -- for GD319 the 2.5" separation is sufficient to avoid serious interference of the companion with the sky region, so no changes were made. However, Vela I has a separation of only 1" so we used a larger sky annulus with inner and outer radii of 40 and 50 pixels, respectively, for the WFC data; this sky region is large enough to encircle both stars and avoid serious contamination from the companion.<sup>1</sup> The resulting count rates are presented in Table 16 above. For the double stars GD319 and Vela I we separately list count rates for the component stars A and B.

The unpolarized star GD319 is especially important as it will be used to determine the instrumental polarization and hence will serve as a corner stone of the calibration. Here we briefly consider whether there is evidence of complications from it being a double star. The count rate ratios for POL60/POL0 and POL120/POL0 are presented in Table 17 for

---

1. We also performed an analysis of GD319 using very large sky apertures which encircled both stars (inner and outer radii of 200 and 230 pixels, respectively, for the HRC and 140 and 285 pixels, respectively, for the WFC). This gave effectively identical polarization results.

each component and for the sum A+B. The uncertainty on the ratios due to photon statis-

**Table 17.** Preliminary Results for GD319

Visit	Detector	Band	Polarizers	Ratio of Count Rates		
				Star A	Star B	Star A + Star B
2	WFC	F475W	POL60V / POL0V	0.972	0.975	0.972
			POL120V / POL0V	1.000	1.005	1.001
		F606W	POL60V / POL0V	0.980	0.977	0.979
			POL120V / POL0V	1.013	1.015	1.014
		F775W	POL60V / POL0V	1.026	1.024	1.025
			POL120V / POL0V	1.016	1.014	1.015
4	HRC	F475W	POL60V / POL0V	1.094	1.089	1.093
			POL120V / POL0V	1.129	1.120	1.127
		F606W	POL60V / POL0V	1.089	1.086	1.088
			POL120V / POL0V	1.105	1.100	1.103
		F625W	POL60V / POL0V	1.068	1.065	1.067
			POL120V / POL0V	1.068	1.063	1.066
		F658N	POL60V / POL0V	1.094	1.091	1.092
			POL120V / POL0V	1.092	1.087	1.089
		F775W	POL60V / POL0V	1.076	1.075	1.075
			POL120V / POL0V	1.044	1.042	1.043
		F435W	POL60UV / POL0UV	1.159	1.168	1.161
			POL120UV / POL0UV	1.108	1.114	1.109
F330W	POL60UV / POL0UV	-	1.141	-		
	POL120UV / POL0UV	-	1.078	-		

tics is about 0.1%. The flat fields also contribute error as the images are not perfectly registered, and there is some noise in the flats for the separate polarizer filters. As we discuss later, this ranges from ~0.2% to ~0.4% depending on the polarizer filter and detector. It appears that the count ratios for star A and star B are generally consistent within the uncertainties. This implies that both stars in the pair are unpolarized (or more strictly, that they at least have the same polarization), and eases our concerns that the ground-based polarimetry for this star (Schmidt, Elston, and Lupie 1992) might be corrupted if their aperture partially excluded light from one or both stars.

## **Proposal 9661 “ACS Polarization Calibration”**

Proposal 9661 (Biretta PI) is the Cycle 11 polarization program. Its purpose is to repeat or supplement problem exposures in 9586, as well as to provide more complete information on the polarizer throughputs. In detail, its objectives are to:

1. Repeat saturated exposures in 9586 using shorter exposure times and/or higher gains (higher electrons/DN).
2. Repeat several good images in 9586 (F606W, F435W, F250W) as consistency check, and to test for change in the polarizers.
3. Take data for a different unpolarized star since GD319 turned out to be a double star -- the new star G191B2B was used for WFPC2 calibration.
4. Take images of the polarization standard stars with and without the polarizers in place, so that the throughputs can be more directly measured. While strictly speaking, polarization depends on the relative measurements between the 0, 60, and 120 filters, the absolute throughput may be very useful in diagnosing anomalies.
5. Take images of polarized stars at different telescope orientations from 9586 so as to remove degeneracies in the calibration and check accuracies of polarization position angles.
6. Take images of NGC104 with and without the polarizers while keeping the target fixed on the CCD, to more directly confirm the polarizer flat fields.

In May 2003 the proposal was de-scoped by management decree from 16 to 9 orbits, and various compromises were made to accommodate this: (i) NGC104 and CRL-2688-2 observations were removed, (ii) some CR-SPLITS were removed, (iii) sometimes the POL filter sequence was changed from 0-60-120 to 120-60-0 to minimize filter wheel overhead times, (iv) visits were changed to single-orbits to optimize buffer dumps, and (v) exposure times were reduced at the expense of signal-to-noise ratio. Below we briefly summarize the visits. Table 18 gives details of the individual exposures.

### ***Visit 3: HRC, polarized star BD+64DEG106, 1 orbit.***

This visit observes a polarized standard star in the HRC in three spectral filters (F250W, F435W, and F606W) crossed with the POL\_V and POL\_UV filters. Its purpose is to provide a second set of data at a different telescope orient from similar observations in program 9586 (goal 4 on page 6), and test for any on-orbit evolution of the calibration (goal 8 on page 7). See notes for program 9586 Visit 3 above.

***Visits 20 & 21: WFC, polarized star Vela, 2 orbits total.***

This essentially repeats Visit 1 of 9586 where three of the six images had been saturated. The new observations use GAIN=4 to avoid saturation of the a-to-d converter. Sub-exposures of 2 sec or longer are used to minimize shutter jitter issues (Gilliland and Hartig 2003). Also included are exposures without the polarizers, so that the absolute transmissions of the polarizers could be measured and compared with pre-launch values (goal 3 on page 6). The observations should also occur at a different HST orientation from Visit 1 of 9586 so as to provide some check of the derived polarization position angles (goal 4 on page 6). See notes for program 9586 Visit 2 above. Two single-orbit visits are used to optimize scheduling of the buffer dumps.

***Visit 40 & 41: HRC, unpolarized star GD319, 2 orbits total.***

This repeats a subset of Visit 4 of 9586 which had many saturated exposures. Specifically F606W and F625W are crossed with the three POL\_V filters. And F220W, F250W, F330W, F435W, and F814W are crossed with the three POL\_UV filters. The primary goal is to assess the instrumental polarization (goals 1 and 2 on page 5). Exposures without the polarizers are included to allow measurement of the absolute throughputs for the polarizers (goal 3 on page 6). See notes for 9586 Visit 4.

***Visit 90 & 91: WFC, unpolarized star G191B2B, 2 orbits total.***

This repeats 9586 Visit 2 using a different star. The previous target GD319 is a double star (2.5" separation) which creates some difficulties in performing aperture photometry, as well as some discomfort about the accuracy of the ground calibration. Here we repeat these observations with a different star, G191B2B, which was used extensively for the WFPC2 polarization calibration. It has been characterized from the ground by Schmidt, Elston, and Lupie (1992) who give polarizations of  $0.065 \pm 0.038$ ,  $0.090 \pm 0.048$ , and  $0.061 \pm 0.038$  percent at U, B, and V bands, respectively. In our calibrations F475W, F606W, and F775W are crossed with the three POL\_V filters. The purpose of these data are primarily to assess the instrumental polarization (goals 1 and 2 on page 5). Images without the polarizers are included to allow measurement of the absolute throughput of the polarizers (goal 3 on page 6). This star is rather bright, so there are trade-offs between avoiding WFC shutter jitter at short exposures<sup>1</sup> and saturation effects at long exposures. We have sometimes included a long exposure which is expected to saturate the CCD full well, but it is believed that these images should still have good photometric accuracy provided the a-to-d converter is not saturated (Gilliland 2004). GAIN=4 is used to avoid saturation of the a-to-d converter.

---

1. WFC shutter jitter primarily impacts exposures times of 2 sec. or less. Non-repeatable errors up to 1% can occur (Gilliland and Hartig 2003).

**Visit 95 & 96: HRC, unpolarized star G191B2B, 2 orbits total.**

This repeats 9586 Visit 4 using a different star G191B2B; see notes for 9661 visits 90 and 91 above. Specifically F475W, F606W, and F775W are crossed with the three POL\_V filters; and F220W, F250W, F330W, F435W, and F814W are crossed with the three POL\_UV filters. The purpose of these data are similar to Visits 95 & 96.

**Exposure List and Preliminary Results**

Table 18 below summarizes the exposures for 9661 and gives the measured count rates for the standard stars. See previous discussion of program 9586 for analysis methods, etc. See *note added in proof* on page 62.

**Table 18.** Summary of exposures for proposal 9661

Visit	Detector	Target	Date	PA_V3 (deg)	Notes
Images	Filter1	Filter2	Exp. Time (s)	Count Rate (e- / s) (Star A / B)	
Visit 3	HRC	BD+64D106	5/13/2003	135.4	
j8mj03011	F606W	POL0V	2	651915	
j8mj03021	F606W	POL60V	2	716861	
j8mj03031	F606W	POL120V	2	662958	
j8mj03041	POL0UV	F435W	8	133022	
j8mj03051	POL60UV	F435W	8	154678	
j8mj03061	POL120UV	F435W	8	136364	
j8mj03071	POL0UV	F250W	200	4259	
j8mj03081	POL60UV	F250W	200	4772	
j8mj03091	POL120UV	F250W	200	4008	
Visits 20 & 21	WFC	Vela	6/13-14/2003	312.0	
j8mj20011	F475W	POL0V	12	18691 / 3366	
j8mj20021	F475W	POL60V	12	20281 / 3617	
j8mj20031	F475W	POL120V	12	20655 / 3758	
j8mj20041	F475W	CLEAR2L	4	53706 / 9603	
j8mj21031	F606W	POL0V	6	60209 / 12193	
j8mj21021	F606W	POL60V	6	65393 / 13280	
j8mj21011	F606W	POL120V	6	66942 / 13545	
j8mj20051	F606W	CLEAR2L	3	164830 / 33145	

**Table 18.** Summary of exposures for proposal 9661

Visit	Detector	Target	Date	PA_V3 (deg)	Notes
Images	Filter1	Filter2	Exp. Time (s)	Count Rate (e- / s) (Star A / B)	
j8mj21ndq	F775W	POL0V	2	72835 / 16741	shutter jitter?
j8mj21neq	F775W	POL60V	2	77210 / 17572	shutter jitter?
j8mj21nhq	F775W	POL120V	2	78964 / 17939	shutter jitter?
j8mj21ncq	F775W	CLEAR2L	2	159002 / 33558	shutter jitter?
Visits 40 & 41	HRC	GD319	7/12/2003	276.2	
j8mj40011	F606W	POL0V	16	58806 / 38167	
j8mj40021	F606W	POL60V	16	64561 / 41581	
j8mj40031	F606W	POL120V	16	65300 / 42008	
j8mj410a1	F606W	CLEAR2S	5.2	168860 / 107824	
j8mj40061	F625W	POL0V	36	29077 / 25539	
j8mj40051	F625W	POL60V	36	31176 / 27123	
j8mj40041	F625W	POL120V	36	31141 / 27104	
j8mj41091	F625W	CLEAR2S	12	82840 / 71357	
j8mj400d1	POL0UV	F220W	130	3669 / -	Star B very faint
j8mj400e1	POL60UV	F220W	130	4351 / -	Star B very faint
j8mj41011	POL120UV	F220W	130	3440 / -	Star B very faint
j8mj410d1	CLEAR1S	F220W	14	59513 / -	Star B very faint
j8mj400c1	POL0UV	F250W	36	10042 / 11.4	
j8mj400b1	POL60UV	F250W	36	11395 / 36.2	
j8mj400a1	POL120UV	F250W	36	9882 / 33.7	
j8mj410c1	CLEAR1S	F250W	6	56953 / 83.3	
j8mj40071	POL0UV	F330W	26	16967 / 322	
j8mj40081	POL60UV	F330W	26	19353 / 340	
j8mj40091	POL120UV	F330W	26	17960 / 346	
j8mj410b1	CLEAR1S	F330W	6	59308 / 1153	
j8mj41041	POL0UV	F435W	24	35831 / 5387	
j8mj41031	POL60UV	F435W	24	41525 / 6230	
j8mj41021	POL120UV	F435W	24	39491 / 5930	
j8mj410e1	CLEAR1S	F435W	6	117767 / 17609	

**Table 18.** Summary of exposures for proposal 9661

Visit	Detector	Target	Date	PA_V3 (deg)	Notes
Images	Filter1	Filter2	Exp. Time (s)	Count Rate (e- / s) (Star A / B)	
j8mj41051	POL0UV	F814W	30	24520 / 43794	
j8mj41061	POL60UV	F814W	30	26709 / 47244	
j8mj41071	POL120UV	F814W	30	25047 / 44952	
j8mj41081	CLEAR1S	F814W	10	45531 / 78484	
Visits 90 & 91	WFC	G191B2B	8/29/2003	91.2	
j8mj91q8q	F475W	POL0V	2	216019	
j8mj90psq	F475W	POL60V	2	209950	
j8mj90pqq	F475W	POL120V	2	216536	
j8mj91qlq	F475W	CLEAR2L	0.5	609946	shutter jitter?
j8mj91qmq	F475W	CLEAR2L	3	617956	> full-well
j8mj90pfq	F606W	POL0V	1.5	241853	shutter jitter?
j8mj90peq	F606W	POL0V	12	240597	> full-well
j8mj90piq	F606W	POL60V	1.5	237967	shutter jitter?
j8mj90phq	F606W	POL60V	12	235428	> full-well
j8mj90plq	F606W	POL120V	1.5	245374	shutter jitter?
j8mj90pkq	F606W	POL120V	12	244644	> full-well
j8mj90pmq	F606W	CLEAR2L	0.5	626519	shutter jitter?
j8mj90pnq	F606W	CLEAR2L	3	640683	> full-well
j8mj91011	F775W	POL0V	4	85807	
j8mj91021	F775W	POL60V	4	83378	
j8mj91031	F775W	POL120V	4	84905	
j8mj91qkq	F775W	CLEAR2L	2	171012	near full-well
Visits 95 & 96	HRC	G191B2B	8/30/2003	90.6	
j8mj95061	F475W	POL0V	6	119621	
j8mj95051	F475W	POL60V	6	130678	
j8mj95041	F475W	POL120V	6	134270	
j8mj960b1	F475W	CLEAR2S	2	374430	
j8mj95011	F606W	POL0V	6	138556	
j8mj95021	F606W	POL60V	6	151884	

**Table 18.** Summary of exposures for proposal 9661

Visit	Detector	Target	Date	PA_V3 (deg)	Notes
Images	Filter1	Filter2	Exp. Time (s)	Count Rate (e- / s) (Star A / B)	
j8mj95031	F606W	POL120V	6	153831	
j8mj960a1	F606W	CLEAR2S	2	396940	
j8mj95071	F775W	POL0V	30	40225	
j8mj95081	F775W	POL60V	30	43253	
j8mj95091	F775W	POL120V	30	41863	
j8mj960c1	F775W	CLEAR2S	10	87425	
j8mj96011	POL0UV	F220W	20	11634	
j8mj96021	POL60UV	F220W	20	13594	
j8mj96031	POL120UV	F220W	20	10800	
j8mj960f1	CLEAR1S	F220W	6.6	191562	
j8mj96061	POL0UV	F250W	15	30860	
j8mj96051	POL60UV	F250W	15	34412	
j8mj96041	POL120UV	F250W	15	30028	
j8mj960g1	CLEAR1S	F250W	5	174474	
j8mj950f1	POL0UV	F330W	15	48776	
j8mj950e1	POL60UV	F330W	15	55150	
j8mj950d1	POL120UV	F330W	15	51299	
j8mj960e1	CLEAR1S	F330W	5	168783	
j8mj950a1	POL0UV	F435W	10	89415	
j8mj950b1	POL60UV	F435W	10	103767	
j8mj950d1	POL120UV	F435W	10	99206	
j8mj960d1	CLEAR1S	F435W	3.2	292895	
j8mj96zoq	POL0UV	F814W	5	55919	
j8mj950g1	POL0UV	F814W	10	55962	
j8mj96071	POL60UV	F814W	10	61041	
j8mj96081	POL120UV	F814W	10	57460	
j8mj96091	CLEAR1S	F814W	4	104729	

## **Proposal 10055 “ACS Polarization Calibration”**

Proposal 10055 (Biretta PI) was designed to study the polarization calibration as a function of HST roll angle, and further study its dependence on position within the ACS field-of-view. This program will execute throughout Cycle 12. The program totals 13 orbits. We give a brief summary of the planned visits:

### ***Visit 10: WFC, polarized star Vela, 4 orbits.***

This visit observes a polarized standard star in the WFC at the field center and at four positions near the edges of the unvignetted field. F606W is used with the three POL\_V filters.

### ***Visit 20: WFC, polarized star Vela, 1 orbit.***

This essentially repeats the field center observation of Visit 10, but with the telescope rolled by 60 degrees.

### ***Visit 30: WFC, polarized star Vela, 1 orbit.***

This essentially repeats the field center observation of Visit 10, but with the telescope rolled by 120 degrees.

### ***Visit 40: HRC, polarized star BD+64DEG106, 2 orbits.***

This visit observes a polarized standard star in the HRC at the field center and at three positions near the field edges. Observations are made in both the F606W+POL\_V and F330W+POL\_UV filter sets.

### ***Visit 50: HRC, polarized star BD+64DEG106, 1 orbit.***

This visit repeats the center position in Visit 40 with HST rolled 60 degrees from that visit. A fourth (new) field position is also added. Observations are made in both the F606W+POL\_V and F330W+POL\_UV filter sets.

### ***Visit 60: HRC, polarized star BD+64DEG106, 1 orbit.***

This visit repeats the center position in Visit 40 with HST rolled 120 degrees from that visit. Again, observations are made in both the F606W+POL\_V and F330W+POL\_UV filter sets. Some measurements near the field edges from Visit 40 are also repeated to fill the orbit and provided a repeatability check.

***Visit 70: HRC, core of star cluster NGC104 (47 Tuc), 2 orbits.***

This visit observes a weakly polarized star cluster with the HRC for a few representative filters. The filters F250W, F330W, F435W are crossed with the three POL\_UV filters; and F606W and F775W are crossed with the three POL\_V filters. The purpose of these data are to test the accuracy of the polarization calibration across the HRC field-of-view, and to measure the wavelength-dependent geometric distortion contributed by optical power in the polarizer filters. A new feature of these observations, is that unpolarized images are included at the same HST roll angle, so that distortions can be mapped across the entire field (i.e. without “losses” in the corners where no stars are mutually available in the polarized and unpolarized images). The exposure times of the polarized and unpolarized images are also better matched, so that more of the stars may be used. A roll angle is chosen roughly 90 degrees to that used for similar observations in program 9586, so as to provide additional information on the field-dependence of the derived position angles (the cluster is polarized at about the 1/2% level).

***Visit 80: WFC, outer region of star cluster NGC104-OUTER (47 Tuc), 1 orbit.***

This visit observes a weakly polarized star cluster with the WFC for F606W crossed with the POL\_V filter set. The goals are similar to Visit 70 for the HRC, and again unpolarized images are included with careful matching of the exposure times. Unlike Visit 70 the roll angle is chosen to be identical to that for similar observations in program 9586. There is also an unpolarized image in F475W, which will be used to aid analysis of the F475W data in program 9586.

## **7. Discussion**

We now consider two issues which are of key importance to the calibration -- the angles of the polarizer filter E-vectors on the sky, and the instrumental polarization.

## Polarizer Angles

We have derived the directions of the polarizer electric vectors on the sky via two methods -- the ACS design specifications, and data from the August 2001 RAS/Cal test. We now compare and discuss the results in detail (Table 19).

**Table 19.** Polarizer Angles from ACS Design and RAS/Cal Test.

Camera	Polarizer	E-Vector Angle on Sky CCW from +V3 Axis (degrees) <sup>a</sup>		Filter Used in RAS/Cal Test
		ACS Design	RAS/Cal Test	
HRC	POL0V	110.6±1.0	(117.03±0.87)	F625W
	POL60V	170.6±1.0	-	-
	POL120V	230.6±1.0	-	-
	POL0UV	110.6±1.0	-	-
	POL60UV	170.6±1.0	-	-
	POL120UV	230.6±1.0	-	-
WFC	POL0V	-38.2±1.0	(-39.49±0.18)	F625W
	POL60V	21.8±1.0	(28.30±0.35)	F625W
	POL120V	81.8±1.0	(78.11±0.27)	F625W
	POL0UV	-38.2±1.0	-38.42±0.39	F814W
	POL60UV	21.8±1.0	22.64±0.37	F814W
	POL120UV	81.8±1.0	81.85±0.37	F814W

a. Values in parenthesis are considered suspect for various reasons -- see text. RAS/Cal uncertainties do not include those from spurious polarization.

The filter angles derived from the ACS design have the advantage of not being subject to spurious polarization or measurement errors, though of course, there is no guarantee that the filters were actually mounted at the correct angles. The ACS design angles show small differences in results (1.6 degrees) depending on whether the drawing of the HRC or WFC was used (method #1 in Table 5, vs. method #2 in Table 6). In Table 19 we give the average of the values derived from the HRC and WFC drawings, and used the difference as an indication of the uncertainty. For example, for the HRC with the POL0V filter, averaging the values from Table 5 and Table 6 shows the PA of the electric vector on the sky is (PA\_V3-69.4) degrees, or equivalently (PA\_V3+110.6) degrees. In other words, the angle

from the +V3 axis to the POL0V electric vector direction is  $110.6 \pm 1.0$  degrees, which is the value we give in Table 19.

The RAS/Cal test, while providing a valuable independent confirmation of the filter angles, is potentially subject to spurious polarization effects in both ACS and RAS/Cal.

As discussed earlier, the RAS/Cal results for WFC with F625W + POL\_V shows anomalous *relative* polarizer angles when compared to the expected 60 degree rotations between filters (Table 13). In addition, the relative intensities for these data are also anomalous (Figure 7 on page 30), which would also be consistent with spurious polarization effects. Not surprisingly, the *absolute* angles from the RAS/Cal test for WFC with POL\_V+F625W (Table 19) show significant disagreement with the ACS design angles. While there is reasonable agreement for POL0V, both POL60V and POL120V disagree with the design angles. Given there is both departure from the expected 60 degree rotations, and evidence for spurious polarization effects in the intensities, we consider the RAS/Cal results for WFC with POL\_V in Table 19 as suspect.

The RAS/Cal results for WFC with F814W+POLUV, in contrast, do not show significant anomalies -- the relative angles in Table 13 are close to the expected 60 degree increments, and the intensities for the three filters in Figure 7 are similar as they should be. This detector/filter combination furthermore shows excellent agreement between the RAS/Cal absolute angles and the ACS design specs (Table 19) -- the values for POL0UV, POL60UV, and POL120UV all agree well within the uncertainties. For example, the design specs give  $-38.2 \pm 1.0$  degrees for the POLUV filter, while the RAS/Cal test gives  $-38.42 \pm 0.39$  degrees. This gives some confirmation that the angles derived from the ACS design specs are accurate.

Unfortunately, there is only one RAS/Cal angle for the HRC with POLV+F625W and it does not agree with the value expected from the ACS design. In Table 19 we see that HRC with POL0V gives an angle  $\sim 7$  degrees larger in the RAS/Cal test than expected from the design specs. Given the problems discussed above for WFC with POLV+F625W, this is perhaps not surprising. Since there is HRC data in only one of the three POL\_V filters, we cannot test for the nominal 60 degree rotations between filters, and hence we consider this one data point for the HRC as suspect (or at least unsupported by other evidence).

Given this extra information, we review again our previous list of options for the RAS/Cal polarizer angle anomalies:

1. One or more of the POLV filters are mounted in the filter wheel at the wrong angle. Given that HRC / POL0V + F625W shows a  $\sim 7$  degree anomaly, while WFC with the same filters shows reasonable agreement, we can rule out incorrect mounting of the filters as the sole cause of the anomaly, since the POL0V filter cannot have two different rotations. This is not to say, however, that there could not be multiple

errors. For example, an error in calculating all the ACS design angles for the HRC plus incorrect mounting of the filters cannot be ruled out.

2. The F625W filter is somehow anomalous, possessing either internal polarization or birefringence, since all the anomalous data seem to be taken in this filter. This remains an attractive, though worrisome possibility.
3. There is a large and unexpected source of polarization within the WFC with a very strong wavelength dependence. This would explain the anomalous results in F625W but normal results in F814W. This seems a little less likely now, since the independent HRC optical chain would need a similar issue to account for the HRC / POL0V + F625W anomaly.
4. There is some measurement error which impacts only the F625W data, but not the F814W data. This seems a little over-conspired, but not impossible.

Of these four, we believe (1) and (3) appear unlikely as single-cause scenarios for the anomalous RAS/Cal polarizer angles. Option (2), a polarization effect in the F625W filter, appears to be the simplest and perhaps most likely cause, followed by option (4), measurement error.

*Given the possibility that the RAS/Cal data might be corrupted by various spurious polarization effects, we recommend using the ACS design spec angles in Table 19 until better information becomes available.*

We anticipate that future on-orbit observations will provide further confirmation of the polarizer angles, and perhaps improved values. Another source of information on the polarizer angles may come from maps of the polarizer geometric distortion. Preliminary distortion maps show numerous small scale features which are attributable to the mechanical stretching applied to the polarizing material during their manufacturing. The small scale distortion features all have a preferred direction which is probably related to the stretch and hence the polarizer E-vector direction. Further study of this effect is left to the future. It is also possible that more information might be recovered from the RAS/Cal data by detailed modeling of the anomalies, but this is beyond the scope of the present report.

## **Instrumental Polarization**

In the absence of instrumental polarization, we would expect each of the polarizers (POL0xx, POL60xx, and POL120xx) to give equal count rates for an unpolarized star. The extent to which this is not true is an indication of the instrumental polarization. The most reliable information on instrumental polarization is likely to come from our on-orbit observations of unpolarized stars. Using the count rates  $r(POLnxx)$  measured for an

unpolarized target at each of the three polarizer angles ( $n=0, 60,$  and  $120$  degrees), the effective Stokes parameters contributed by instrumental effects may be computed as

$$I = \left(\frac{2}{3}\right)[r(POL0V) + r(POL60V) + r(POL120V)]$$

$$Q = \left(\frac{2}{3}\right)[2r(POL0V) - r(POL60V) - r(POL120V)]$$

$$U = \left(\frac{2}{\sqrt{3}}\right)[r(POL120V) - r(POL60V)]$$

The instrumental polarization  $P$  is then given by

$$P = \frac{\sqrt{Q^2 + U^2}}{I}$$

Values of  $P$  derived from the on-orbit programs 9586 and 9661 are given in Table 20 and plotted in Figure 8 and Figure 9. And finally, an angle  $\theta$  associated with the instrumental polarization can be computed as

$$\theta = \left(\frac{1}{2}\right)\text{atan}\left(\frac{U}{Q}\right)$$

Angles defined this way are relative to the E-vectors of the POL0V and POL0UV filters. Values of  $\theta$  derived from the on-orbit programs 9586 and 9661 are also given in Table 20.

The uncertainties on the instrumental polarizations are dominated by the flatfields. The noise in the flats appears to have several components which will affect the images in different ways. Differencing HRC flats for the different polarizer filters (e.g. POL0V - POL60V) shows pixel-scale fluctuations with an RMS of 0.30%. In general we expect the polarizer filters to contribute only large-scale features to the flats, and hence this pixel-scale fluctuation most likely represents a noise due to some polarizer-dependent ingredient in the flats. Another noise component appears to be related to the spectral filter component of the flats -- it appears as a 0.55% RMS fluctuation among adjacent pixels. Some of this could be real variations in the pixel-to-pixel sensitivity of the CCD, however if we difference flats from different spectral filters we find about the same RMS. Assuming there are no large filter-to-filter changes in the CCD pixel sensitivities, we can thus infer that much of the 0.55% RMS must be noise, rather than real features. These two noise components, polarizer-dependent and spectral filter-dependent, affect the images in different ways. The

POLUV filters show a large image shift between the three polarizers, typically around 10 HRC pixels<sup>1</sup>, so these will suffer from a combination of both errors, or around

$$\frac{\sqrt{0.30^2 + 0.55^2}}{\sqrt{2}} = 0.44$$

percent RMS, which leads to an uncertainty in the instrumental polarizations of 0.4%<sup>2</sup>. The POLV images show much better alignment, typically around 1 HRC pixel shift between the polarizers, and so will be impacted mainly by the former error (noise between different polarizers with 0.3% RMS), or an error of

$$\frac{0.30}{\sqrt{2}} = 0.21$$

percent RMS for each polarizer, which leads to an uncertainty in the instrumental polarizations of 0.2%.<sup>3</sup> Hence the uncertainties for the HRC+POLUV instrumental polarizations are ~0.4%, while those for HRC+POLV are ~0.2%. The polarizer flats for the WFC appear to be slightly noisier, and hence the uncertainties for WFC+POLV are ~0.3%.

- 
1. The shift is repeatable and probably arises from a wedge in the POLUV filters.
  2. The root-two arises from initially differencing images to measure the RMS noises. The impact on the polarization is estimated from empirical tests. We may be over-estimating the uncertainty somewhat when the PSF is large enough to encompass many pixels containing uncorrelated noise.
  3. Uncertainties on the instrumental polarization are computed by a Monte-Carlo technique.

**Table 20.** Instrumental polarizations derived from on-orbit data.

Camera	Polarizer	Filter	Target	Program	Inst. Pol. P (%) <sup>a</sup>	Angle $\theta$ (deg.) <sup>b</sup>	Notes
HRC	POLUV	F220W	GD319	9586	(13.1)	(-50.3)	Saturated
			GD319	9661	14.3	-53.0	-
			G191B2B	9661	13.8	-51.5	-
		F250W	GD319	9586	(8.0)	(-54.8)	Saturated
			GD319	9661	9.2	-57.6	-
			G191B2B	9661	8.5	-54.9	-
		F330W	GD319	9586	(6.9)	(-71.7)	Saturated
			GD319	9586	8.2	-77.5	Star B only
			GD319	9661	7.6	-72.5	-
			G191B2B	9661	7.2	-71.6	-
		F435W	GD319	9586	8.7	-80.5	-
			GD319	9661	8.5	-79.7	-
	G191B2B		9661	8.7	-80.9	-	
	F814W	GD319	9586	4.7	-68.9	-	
		GD319	9661	4.7	-68.5	-	
		G191B2B	9661	5.2	-68.3	-	
	POLV	F475W	GD319	9586	7.1	82.6	-
			G191B2B	9661	6.9	83.2	-
		F606W	GD319	9586	6.1	86.2	-
			GD319	9661	6.3	87.0	-
			G191B2B	9661	6.5	86.6	-
		F625W	GD319	9586	4.2	-89.6	-
	GD319		9661	4.3	-89.6	-	
	F658N	GD319	9586	5.8	-89.4	-	
F775W	GD319	9586	4.2	-77.4	-		
	G191B2B	9661	4.2	-76.4	-		
WFC	POLV	F475W	GD319	9586	1.9	30.8	-
			G191B2B	9661	2.0	32.0	-
		F606W	GD319	9586	2.0	41.7	-
			G191B2B	9661	2.2	43.0	-
		F775W	GD319	9586	1.4	18.8	-

Camera	Polarizer	Filter	Target	Program	Inst. Pol. P (%) <sup>a</sup>	Angle $\theta$ (deg.) <sup>b</sup>	Notes
			G191B2B	9661	1.7	19.2	-

- a. Uncertainties are ~0.4% for HRC+POLUV filters, ~0.2% for HRC+POLV filters, and ~0.3% for WFC+POLV filters.
- b. Angle is relative to the zero-angle polarizer (POL0V or POL0UV). Uncertainties on the angles are approximately given by  $30(\text{inst pol uncertainty})/(\text{inst pol})$  in degrees.

The instrumental polarization for the HRC is shown in Figure 8. The on-orbit measurements for proposals 9586 and 9661 (unpolarized targets GD319 and G191B2B) are all in excellent agreement with each other. This agreement mitigates previous concerns that the data for double star GD319 in program 9586 might be somehow corrupted, since it gave values significantly larger than the RAS/HOMS pre-launch test. The instrumental polarization appears to be lowest at the red end (F814W) with values around 5%, and then increases steadily towards the blue end of the spectrum. In the ultraviolet there is a sharp rise to a maximum of 14% at F220W.

The F625W filter appears to be somewhat anomalous. It is about 2% lower than adjacent F606W and F658N. We have already noted some anomalous behavior in this filter during the RAS/Cal test. This could occur if the F625W filter were birefringent, and hence converting some of the incident linearly polarized light into circularly polarized light. This circularly polarized component would then pass into the linear POLV filters where it registers as unpolarized light, thus apparently reducing the overall system polarization.<sup>1</sup> We also note that F330W is lower than F435W, which goes against the overall trend, but it is not clear whether this indicates some anomaly, or some discontinuity between these POLUV data and the POLV data at longer wavelengths.

Also plotted is the polarization expected from the HRC M3 mirror in isolation. While this mirror can account for all of the polarization at the red end of the spectrum, there are clearly other sources of polarization that become important by 6000 Angstroms, and completely dominate at shorter wavelengths. These other sources probably include the CCD detector, other mirrors, and possibly anomalies in the spectral filters. The dotted line in the figure shows a very crude attempt to model the combined instrumental polarization of the M3 mirror together with the CCD. Here we have modeled the CCD as a silicon surface which is tilted by 30.8 degrees, and assumed M3 and the CCD are tilted about parallel axes. While our model for the CCD is certainly over-simplified, it at least has some simi-

---

1. While this apparent reduction of instrumental polarization in F625W seems like a good thing, the birefringence would in fact have a devastating effect on observations of polarized targets.

larity to the on-orbit data and reproduces the increase in instrumental polarization towards the blue end of the spectrum.

Results of the pre-launch RAS/HOMS test are also plotted. These do not agree very well with the on-orbit data, and we attribute this to spurious polarization in the RAS/HOMS optics. As mentioned before, the two mirrors in RAS/HOMS are expected to contribute a spurious 6% polarization, which is enough to account for the differences from the on-orbit data. It is also possible that some of the disagreement arises from comparing a point source test (on-orbit standard star) against a flat field test (RAS/HOMS). In the later case, there would be more scattered light arriving at the CCD detector, with a potential to reduce the measured polarization.

The HRC design goal of 5% between 220 and 1000 nm is also indicated<sup>1</sup>. This goal appears to have been met for F625W, F775W, and F814W, but not for filters at shorter wavelengths. The instrumental polarization budget for the instrument design appears to have been set based on models for the M3 mirror (Woodruff 1996C); effects in the tilted CCD appear to have been ignored.

Figure 9 shows the instrumental polarization for the WFC. In general, the instrumental polarizations are much lower than for the HRC. The on-orbit observations in programs 9586 and 9661 are again in good agreement with each other, and show values between ~1.5% and 2%. As before, the RAS/HOMS data are in poor agreement with the on-orbit data, which we believe is caused by a large polarization in the RAS/HOMS optics.

As with the HRC M3 mirror, we have tried to model the instrumental polarization due to the WFC IM3 mirror alone, and the IM3 mirror combined with a simple model of the 20.2 degree tilted WFC CCD. At F606W the model with the CCD appears to be better than a model with just the IM3 mirror alone, but at F475W they are about equally in error. The lab measurements for the IM3 mirror witness sample only extended to 7000 Angstroms, so we cannot reliably model beyond that (the mirror coating is proprietary and difficult to calculate reliably).

The design goal for the WFC of 1% instrumental polarization appears not to have been met. Again, the goal was based solely on the properties of the mirrors, and did not include effects from the CCD.

As with the instrumental polarization values, the polarization angles  $\theta$  in Table 20 appear to be in good agreement across different targets and proposals. The angles for the HRC appear to vary smoothly with wavelength. The smallest angles are at the ends of the spectrum, near -52 degrees at F220W and -68 degrees at F814W. The largest angles occur in

---

1. The Contract End Item Specification (Nov. 1995) is for a maximum allowed value of 6.5% between 220 and 1000 nm (also Ford, et al., 1996).

the middle of the spectrum with values near -97 degrees (equivalently +83 degrees in Table 20) for F475W. Detailed analyses of these angles is beyond the scope of the present report, but we will briefly comment: if the M3 mirror were the only source of instrumental polarization in the HRC, we would expect the dominance of  $R_s$  longwards of 4000 Angstroms (Figure 5) to produce instrumental polarization roughly parallel to the zero-angle polarizer direction<sup>1</sup>, and hence angles  $\theta$  near zero. The observed angles ranging from -68 to -97 degrees over these wavelengths suggest some other source of instrumental polarization dominates (e.g. the CCD), not the M3 mirror. Angles  $\theta$  for the WFC range from +19 to +43 degrees.

In principal, these values of the instrumental polarization and their corresponding angles can be used to calibrate observer data. Data calibration will be discussed in a forthcoming ISR (Biretta, et al., in preparation).

**Note added in proof:** there is recent (6/14/2004) preliminary evidence that pixel area corrections are being incorrectly applied for data taken using subarrays. If confirmed, this would impact the absolute photometry of the WFC polarization data, and the WFC count rates reported in Table 16 and Table 18. However, since our derived polarization calibrations involve only relative photometry, and since the stars are generally placed at the same detector pixel for the POLnV polarizers, we expect no impact on the polarization results here in.

---

1. Our preliminary modeling of the ACS optics indicates the HRC M3 mirror is tilted about a rotation axis roughly parallel to the E-vector of the POL0V and POL0UV polarizers. More detailed discussion of the camera geometry is left for future reports.

**Figure 8:** Instrumental polarization for the HRC.

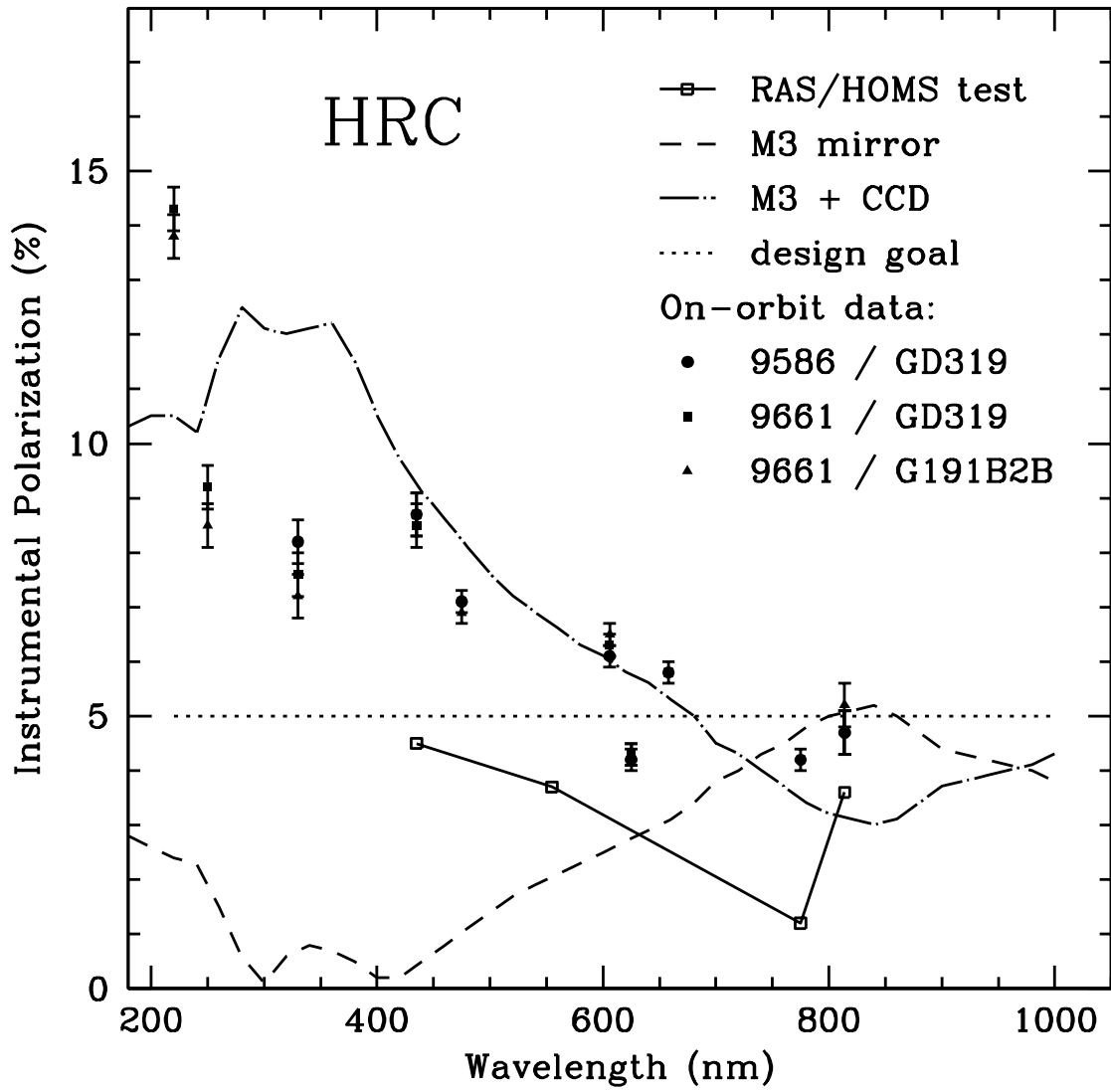
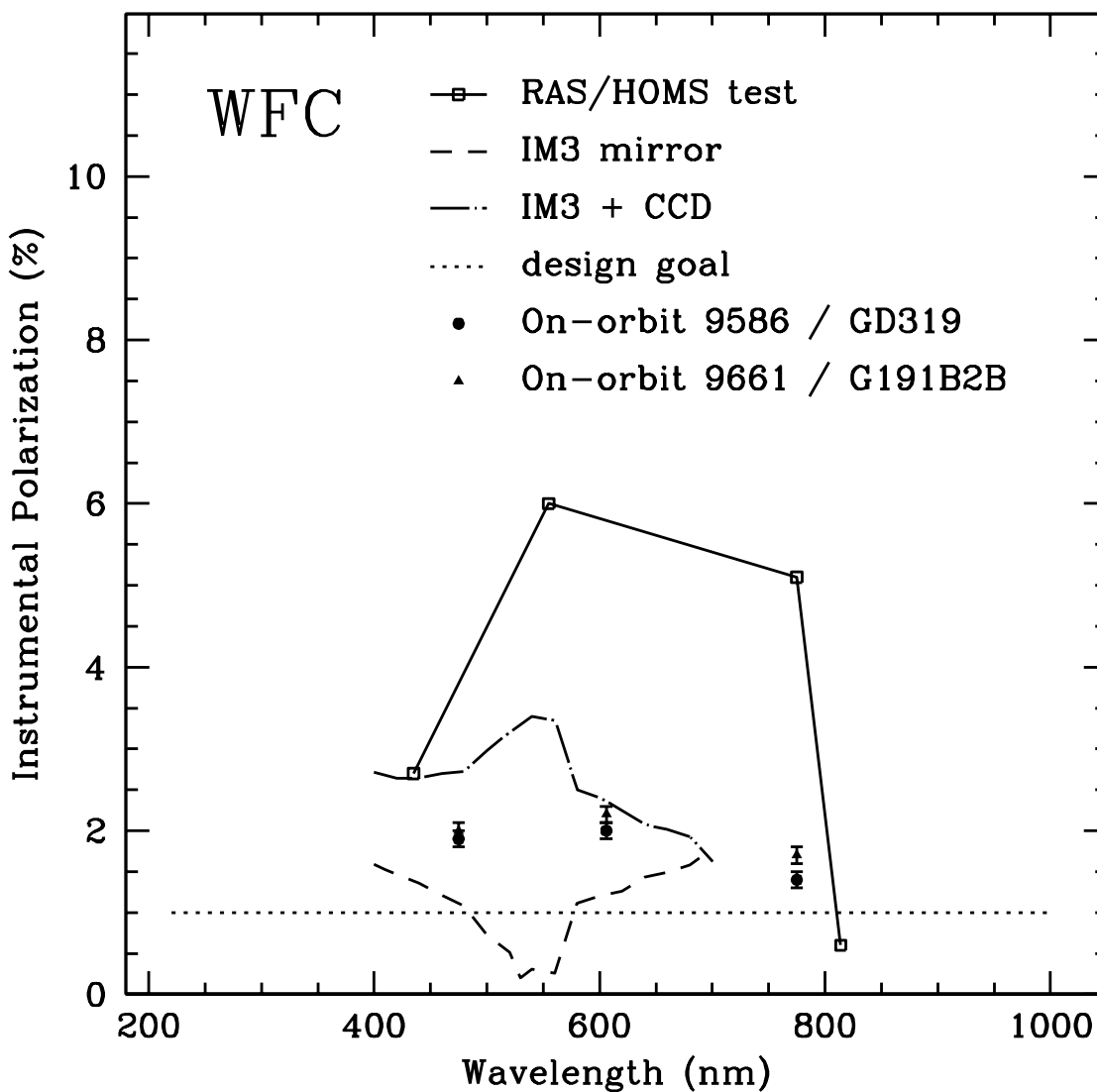


**Figure 9:** Instrumental polarization for the WFC.



## 8. Remaining Issues

There are a number of open issues which must be resolved before ACS polarization data can be calibrated to high accuracy. We briefly discuss these:

1. Phase retardance and far-red performance of the IM3 mirror: The phase retardance was not measured prior to installation of the mirror, and due to the proprietary

nature of the coating, it cannot be accurately calculated. Certain values of the retardance angle could have grave consequences for polarimetry with the WFC. For example, if the retardance were 90 degrees, the instrument would have fairly normal behavior when the target was polarized along one of the principle axes of the IM3 mirror. However, targets polarized near 45 degrees to the principle axes would always appear as unpolarized. This would make the presently favored observing strategy -- observations at one telescope roll angle in POL0, POL60, and POL120, completely unusable. Lower retardance angles will give less extreme effects, but the apparent polarization properties of the target will still be a function of the IM3 mirror rotation on the sky. If the phase retardance were known, it would be fairly straight-forward to model and correct these effects. Lacking this information, it could be derived through more extensive on-orbit calibration. This could be achieved by obtaining WFC images of a highly polarized standard target at many HST roll angles. The far-red properties of the coating are also unmeasured, and hence additional attention might be needed to calibrating WFC polarimetry in the F775W and F814W filters.

2. Far-UV calibration of POL\_UV filters: No measurements of the polarizer filter properties were made shortwards of 2500 Angstroms. This will seriously compromise the ability to calibrate fractional polarizations in F220W and will affect to a somewhat lesser degree data in F250W. This could probably be overcome via observations of highly polarized standard targets in these filters.
3. CCD polarization effects: For a tilted CCD, as we have in both the HRC and WFC, the transmission and reflectivity will be a function of the polarization properties of the incident light. Hence the CCD detection efficiency will depend on the polarization properties of the incident light. This is probably a minor issue for the POL\_V filters -- since the cross-polarized transmission is essentially zero, the CCD effects will merely appear as a small adjustment in the "gain" of each polarizer filter. However, if there is significant leakage of cross-polarized light, as there is with the POL\_UV filters, there is the potential for a very complex interaction of the target's polarization properties with the CCD detector properties. This would add another level of complication to the calibration where the system "gain" depended on the target properties. It appears that this issue has never before been addressed in astronomy<sup>1</sup>, and no pre-launch tests of the CCD's polarization properties were made. It may be possible to compute these effects, but detailed proprietary information on the CCD construction would be needed. Alternatively, it could be calibrated on-orbit by observing polarized targets at many HST roll angles.
4. Confirmation of the POL\_V filter angles: Most of the results for the POL\_V filter angles in the RAS/Cal test appear anomalous. While we believe the problem is not the POL\_V filters, it would be nice to have an on-orbit confirmation of the filter angles.

---

1. ACS is probably the first polarimeter with tilted CCDs.

5. F625W anomalies: There is some evidence in both the RAS/Cal test and the instrumental polarization results for anomalies in the F625W filter. This could arise from birefringence or polarization in the spectral filter itself. It appears that there were no filter specifications or filter test for these effects prior to launch. This type of phenomenon will greatly complicate the calibration, as we can no longer assume similarity between filters at similar wavelengths; each filter would need its own full-up calibration.

## 9. Advice for Observers

If one has some freedom in choosing detectors and filters, it would appear that the greatest chance for success will come with using the HRC with the POLV filters. This is because the properties of the M3 mirror appear to be well-known. In addition, the POLV filters have a very high rejection of cross-polarized light, thus simplifying the calibration.

Using the WFC is somewhat more risky, at least at this point in time, since the properties of the IM3 mirror are poorly known. While its lower instrumental polarization is attractive, there is some danger that a high phase retardance could make the data very difficult, if not impossible, to calibrate.

Some filters should probably be avoided, at least until more information is available. These include F220W and F250W, where the POLUV throughputs were not measured prior to launch. Also the F625W filter, which looks anomalous in both the RAS/Cal test and in the instrumental polarization results. And also the WFC with F775W and F814W since there is no data for the IM3 mirror at these wavelengths.

Observers who are not doing polarimetry should be aware that instrumental polarization will corrupt their data, too, *if the target is polarized*. For example, a target which is 10% polarized will suffer a 3% variation in the measured flux at F220W as the HST roll angle is varied. A more extreme example might be an optical jet in an active galaxy -- a feature with 50% polarization would suffer 14% brightness variation with the HST roll angle! Accurate intensity measurement in these situations will require full polarization measurements, so that polarization effects can be properly assessed and corrected.

## 10. Future Plans

We briefly summarize near- and long-term plans for the polarization calibration:

1. Derive preliminary polarimetric calibration for observers based on results in this report.

2. Obtain data on a polarized standard at several HST roll angles to test for higher-order effects in the calibration (planned for calibration program 10055).
3. Obtain data on a highly polarized target at many HST roll angles to calibrate the interaction between roll angle and computed fractional polarization (phase retardance effects, polarizer leakages, etc.).
4. Measure field dependence of calibration using 47 Tuc and observations of a polarized standard at several field positions (existing data and new data planned for program 10055).
5. Measure polarizer geometric distortions using 47 Tuc data; update calibration pipeline as needed. Obtain 47 Tuc data for more filters (calibration program 10055).
6. Obtain more information for proprietary coatings on the WFC IM3 mirror and CCDs, and attempt to model their effects.
7. Perform laboratory tests on the IM3 and M3 mirror flight spares to quantify their phase retardance effects. Perform lab tests on the CCDs at appropriate tilt angles to measure polarization effects. (There are currently no plans to do this; presumably substantial funding would be required.)
8. Create a model of the ACS optical chain with full polarization effects using Mueller matrices (similar to Biretta and McMaster 1997, and extending the work of Walsh 2001). Compare model and available data for standard stars to see how well the instrumental effects can be predicted. We would likely need to use on-orbit data to solve for properties of the optics, since the pre-launch calibrations were inadequate or incomplete in several areas. We would then package model in user-friendly form for release to observers.
9. Repeat several basic calibrations in future cycles to test for any changes in the polarizers.

## 11. Summary

We have reviewed the current status of the ACS polarization calibration. We began with a brief description of the instrument and the GO science program, and then reviewed both pre-flight and on-orbit calibrations.

Polarizer throughputs were reviewed and slightly revised. Polarizer angles on the sky are computed from both the ACS design specifications and the RAS/Cal ground test. The design and RAS/Cal angles are in good agreement for the POLUV+F814W, but not for the POLV+F625W where differences up to 7 degrees are seen. The reasons for this are poorly understood, but likely causes are unexpected polarization effects in the F625W filter, or RAS/Cal measurement errors which appear only for F625W.

Polarization properties are computed for both the HRC M3 and WFC IM3 mirrors, which are important due to their 47.9 and 49.6 degree incidence angles, respectively. The prescription of the M3 coating is known, and the measured and calculated reflectances are in reasonable agreement. Its calculated polarization is 5% or less, depending on wavelength. Phase retardance effects, however, appear significant -- the calculations show the largest retardance is ~145 degrees near 5800 Angstroms, and will cause a ~33% loss in linear polarization. Unfortunately, the coating prescription of the WFC IM3 mirror is proprietary and therefore its polarization effects are difficult to model. The measured reflectivities imply less than 2% polarization, but the lack of any information regarding the phase retardance is a concern.

On-orbit calibration programs 9586, 9661, and 10055 are described in detail, and preliminary photometry is given for the first two programs. We have used this data to estimate the instrumental polarization and find there is good agreement between the two unpolarized stars and between different observations made at different times for the same star. There is, however, sharp disagreement between this on-orbit data and the RAS/HOMS pre-launch test. We have modeled the RAS/HOMS optics, and predict a large spurious polarization within the lab test instrument, which may account for the disagreement with the on-orbit tests.

The on-orbit data show around 5% instrumental polarization in HRC in the far red, which increases to 14% in the far-UV. These higher numbers are difficult to understand unless there is a large unexpected source of spurious polarization within the HRC. The 31 degree tilt of the CCD detector appears to be the most likely source, and a crude model of the CCD accounts for much of the increase towards the blue and UV. The WFC shows ~2% instrumental polarization between F475W and F775W.

There are many remaining issues. Among these are the lack of information about the WFC IM3 mirror -- the proprietary coating, lack of reflectivity measurements in the far-red, and the lack of information about its phase retardance. The lack of information about the far-UV performance of the polarizers will make calibration of those wavelengths difficult. The potential for large polarization effects in the tilted CCD detectors, their proprietary coatings, and the lack of lab polarization measurements, are serious concerns. The hint of polarization problems in the F625W filter is worrisome, as it opens the possibility of polarization effects in other spectral filters as well.

Observers are advised that "safest" mode at this point is probably the HRC + POLV with visible wavelength filters (e.g. F606W with 6% instrumental polarization); this appears to have the least number of unknowns. The WFC has a lower instrumental polarization (2%), but we cannot yet say whether other effects (e.g. phase retardance) might compromise the observations. The large instrumental polarizations sometimes seen (e.g. the HRC in the UV with 14% instrumental polarization) can have impacts beyond polarimetry -- these

will impact the accuracy of non-polarizer observations if the target happens to be polarized.

## References

Beckers, J. M., 1989, "Polarization Effects in Astronomical Spatial Interferometry," SPIE Vol. 1166, 380.

Biretta, J. and McMaster, M., 1997, "WFPC2 Polarization Calibration," WFPC2 Instrument Science Report 97-11

Denton, 1997. Spectrophotometer plots dated 22 July 1997

Ford, H., et al., 1996, "The Advanced Camera for the Hubble Space Telescope," in Space Telescopes and Instruments IV, Proc. SPIE, Vol. 2807, 184

Forte, et al., 2002, AJ 123, 3263

Gilliland, R., and Hartig, G., 2003, "Stability and Accuracy of the HRC and WFC Shutters," ACS Instrument Science Report 2003-03

Gilliland, R., 2004, "ACS CCD Gains, Full Well Depths, and Linearity up to and Beyond Saturation," ACS Instrument Science Report 2004-01

Gracey, R., 1997, Ball System Engineering Report No. OPT-031 "Filter Installation Drawing," 5/28/1997

Hartig, G., and Martel, A., ACS Ground Calibration Log for 21 August 2001.

Hueser, J., 1996, Ball System Engineering Report ACS OPT-020, "Polarization Effects of Contaminant Films on IM3 and M3," dated 4/26/96, Figure 1

Kubalak, D. 2001, fax dated 30 August 2001 to G. Hartig

Martel, A. 2003, private communication

Schmidt, G.D., Elston, R., and Lupie, O., 1992, AJ 104, 1563 (GD319, BD+64DEG106, G191B2B)

Walsh, J., 2001, "Polarization Properties of ACS," Instrument Science Report ACS 2001-01

Instrument Science Report ACS 2004-09

Whittet, et al., 1992, ApJ 386, 562 (Vela)

Woodruff, R. A., 1996A, Ball System Engineering Report No. ACS OPT-11, "Advanced Camera Polarizer Trade-offs," 1/5/1996

Woodruff, R. A., 1996B, Ball System Engineering Report No. ACS OPT-15, "Advanced Camera Polarizer Code-V Predicted Performance," 1/20/1996

Woodruff, R. A., 1996C, Ball System Engineering Report ACS OPT-018, "ACS Polarization Analysis," 3/5/96